PROOF OF CONCEPT DESIGN FOR A REMOTELY POWERED DEEP BRAIN STIMULATION DEVICE

by

Steven Andrew Hackworth

BS, University of Pittsburgh, 2004

Submitted to the Graduate Faculty of

School of Engineering in partial fulfillment

of the requirements for the degree of
Master of Science

University of Pittsburgh

2005

UNIVERSITY OF PITTSBURGH

SCHOOL OF ENGINEERING

This thesis was presented

by

Steven Andrew Hackworth

It was defended on

July 25, 2005

and approved by

J. T. Cain, Professor, Department of Electrical and Computer Engineering

Mingui Sun, Associate Professor, Department of Neurological Surgery

Robert Sclabassi, Professor, Department of Neurological Surgery

Thesis Advisor: Marlin H. Mickle, Nickolas A. DeCecco Professor, Department of Electrical and Computer Engineering

Thesis Co-Advisor: Michael R. Lovell, Associate Dean for Research, School of Engineering

PROOF OF CONCEPT DESIGN FOR A REMOTELY POWERED DEEP BRAIN STIMULATION DEVICE

Steven Andrew Hackworth, MS

University of Pittsburgh, 2005

Parkinson's disease is a neurodegenerative disorder that causes tremor, stiffness, and slowness of movement. The first line of treatment for the disease is the administration of drugs. Over a period of time, these drugs slowly lose their affect to arrest the symptoms associated with Parkinson's disease. Once a patient becomes refractory to drug treatment, one alternative treatment option is Deep Brain Stimulation (DBS). In DBS, a probe is implanted in the basal ganglia area of the brain to administer electric pulses that curb the aforementioned symptoms. Although not fully understood, DBS is becoming a more widely accepted treatment, with various implantable devices currently on the market. These devices, however, require the implantation of a relatively large battery and control pack in the chest with subcutaneous wires threaded up through the neck to the top of the skull. The control pack and wires are a common source of irritation and infection, sometimes necessitating long periods of antibiotics or even removal of the device. Furthermore, the device is susceptible to magnetic interference and has a limited battery life. After the average 3- to 5-year lifespan of an implant's battery, another surgery is required to replace the device. The aim of this research is to design a small remotely powered device capable of driving a DBS probe from directly under the scalp. Successful development and proof of viability will form a basis for the conceptual redesign of currently marketed devices in order to eliminate the intrusive battery pack and wires, as well as the health risks commonly associated with them and the implantation procedure.

TABLE OF CONTENTS

LIST OF TABLES

LIST OF FIGURES

PREFACE

I would like to express my deepest gratitude and appreciation for Dr. Marlin Mickle's support and guidance, without which I would not have had the opportunity to work on such an exciting and visible project. I would also like to thank the founders of E-SOC, whose optimism and eagerness have gone far in fueling this project, both directionally and financially. Additional thanks go to Cam Hick whose logistical help has been invaluable. Finally, recognition goes to my peers in Dr. Mickle's lab, who never fail to provide insightful discussion.

1.0 INTRODUCTION

Parkinson's disease currently affects more than one million people in the United States [1]. Various treatments exist to suppress the symptoms associated with the condition, including Deep Brain Stimulation, or DBS. Many of the details of the disease and treatment are still unknown, but this chapter attempts to give the reader an idea of the mechanisms of Parkinson's disease and DBS to the degree of current scientific knowledge. It serves to highlight the importance of DBS and, more specifically, the need for improving the currently marketed DBS implant.

1.1 BACKGROUND

1.1.1 Parkinson's Disease

Parkinson's disease is a neurodegenerative disorder that affects an area of the brain called the basal ganglia. Symptoms include stiffness, slowness of movement (bradykinesia) and resting tremor, all seemingly resulting from a lack of dopamine. Many likely indirect symptoms such as depression and dementia are also common in many patients. To understand the nature of the disease, the function of the basal ganglia must first be understood. Its various sections and their relative connections are outlined in Figure 1. In this figure, blue arrows correspond to excitatory connections, usually utilizing the neurotransmitter Glutamate, while red arrows correspond to inhibitory connections, usually utilizing the neurotransmitter GABA. Current theory suggests two pathways: a direct pathway and an indirect pathway. For purposes of this analysis, the

striatum, the main control center, will be the start of both of these pathways, taking feedback information from the motor cortex and controlling the magnitude of overall excitation or inhibition.

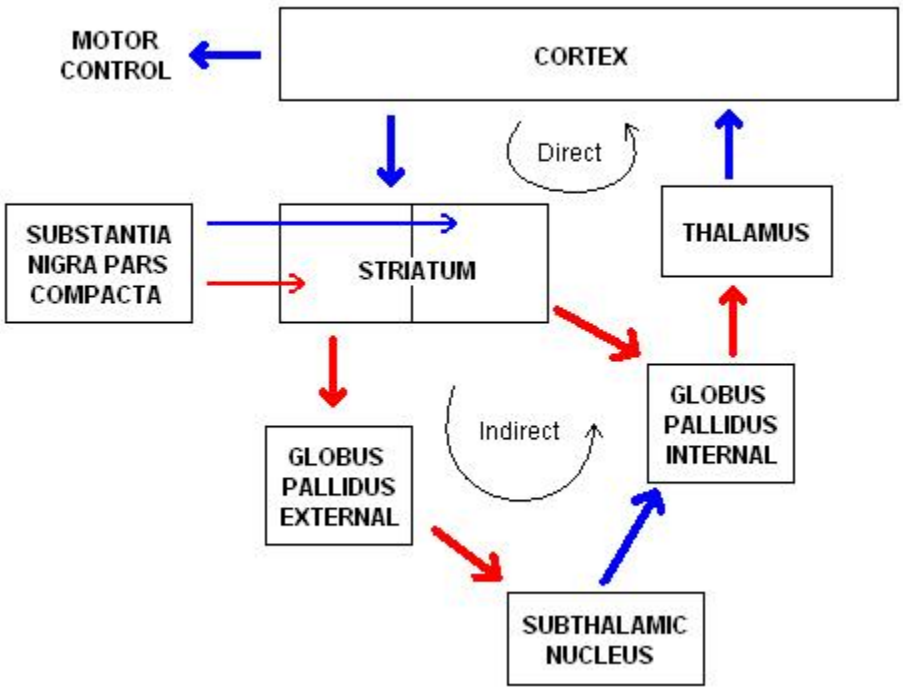

Figure 1: Normal motor control pathway in the basal ganglia.

The entire control system is explained using the "focused selection and tonic inhibition" concept [2]. When a person focuses on an activity, the striatum produces inhibitory outputs to both the direct and indirect pathways. Along the indirect pathway, the globus pallidus external (GPe) is inhibited, which results in a disinhibition of the subthalamic nucleus (STN). The STN's excitatory outputs to the globus pallidus internal (GPi) in turn cause an inhibition of the thalamus, tending to suppress movement, accounting for the "tonic inhibition." Along the direct,

or focused pathway, the striatum output inhibits the (GPi), thus disinhibiting the thalamus whose excitatory stimuli along the direct path allow the intended movement to be performed.

In people with Parkinson's disease the control pathway in Figure 1 is disrupted. Science points to the cause being the depletion of dopamine from the nigrostriatal pathway ([2], [3]) as an effect of the degeneration of the substantia nigra pars compacta (SNc). The actual cause of this degeneration is not certain, though evidence points to a number of possible factors, including environmental toxins, certain drugs and, to a lesser extent, heredity [1]. The effects of SNc degeneration on the basal ganglia control pathway are shown in Figure 2.

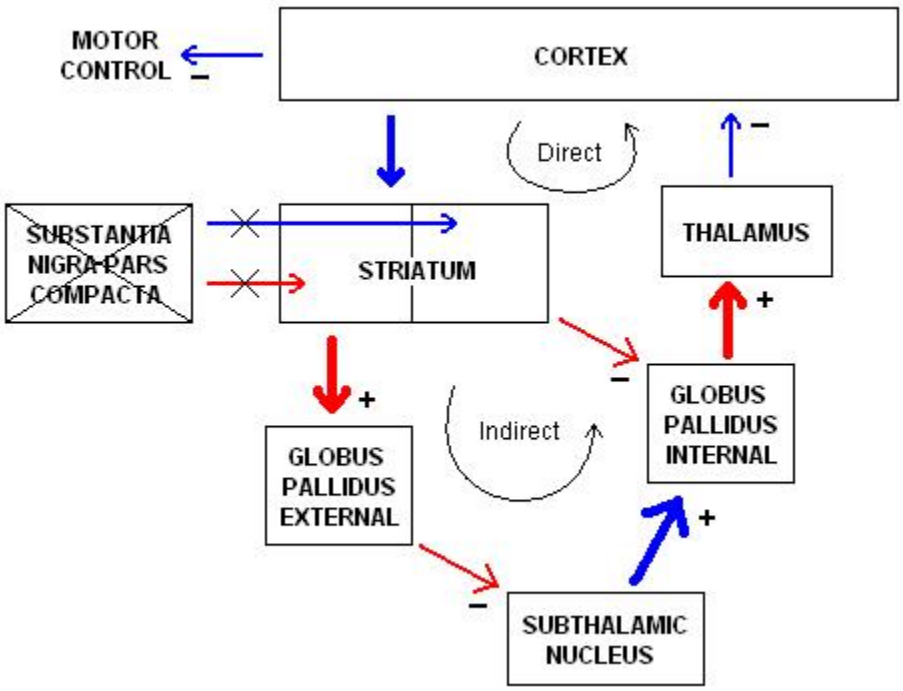

Figure 2: Parkinson's disease motor control pathway.

Examining a directed movement as before, except with this modified control system, illustrates the cause of stiffness and bradykinesia. Without the excitatory input from the SNc, the

striatum's inhibitory output along the direct pathway is reduced, disinhibiting the GPi, thus causing an increased inhibition of the thalamus which results in a reduction of excitatory stimulation to the motor cortex and motor control neurons. Analyzing the indirect pathway gives similar results. Without the inhibitory input from the SNc, the striatum greatly inhibits the GPe, causing a disinhibition of the STN. The overactive STN then greatly excites the GPi, resulting in an even greater inhibition of the thalamus and thus less motor cortex excitation. So, both the direct and indirect paths act on suppressing motor control, preventing intended movement.

The model above does not explain the cause of tremor in patients with Parkinson's disease. Even less is known about the mechanism behind resting tremor, but research points to an oscillatory mechanism somewhere outside of the thalamic region [2]. Also, nuclei associated with transporting signals between the thalamus and cerebellum seem to be connected with the tremors, further supporting the notion of pathways outside the basal ganglia being responsible for tremors.

1.1.2 Deep Brain Stimulation

Various treatments exist for Parkinson's disease, including numerous drugs, brain lesions and deep brain stimulation or DBS. The focus here will remain on DBS which is a form of treatment requiring surgery to implant a probe into the brain and its corresponding controller into the body. Although surgery is considered only after patients become refractory to drug treatments, DBS has become fairly common. The treatment is mainly used for Parkinson's disease, but it can also be used to treat other diseases, such as Hungtington's, dystonia, and epilepsy [2]. Two probes are usually implanted bilaterally into the STN or GPi, where electric pulses are administered to curb the symptoms of stiffness, bradykinesia, and tremor associated with Parkinson's disease.

Although not completely understood, some theories exist as to how DBS actually works. The first theory is that the treatment suppresses neuronal activity via saturation, decreasing output from the pulsed area. The results of DBS in the GPi are similar to those of a pallidotomy, or removal of the GPi, and experiments on DBS in the STN of rats have shown depressed neuronal activity. However, other tests support a different theory, that of increased activity in stimulated centers. Both biological tests and computer simulations support the idea that stimulation regulates neurons, improving data propagation over the irregular neuronal activity present before DBS [2], [3].

Regardless of the actual mechanism of DBS treatment, it proves effective in curbing symptoms associated with Parkinson's disease and improving the quality of life for patients. Further research on the topic is sure to bring new aspects to light, increasing the effectiveness of the procedure.

1.2 CURRENT DBS SHORTCOMINGS

The problems encountered with currently marketed stimulators make them less than ideal as implantable devices. Because of the large battery, the stimulator must be implanted in a separate surgery from that in which the probes are implanted, in order to tunnel and attach the connecting wires to the implant placed under the clavicle. These stimulators are cumbersome in a patient's chest, often causing infection. The infection can require months of antibiotics or even removal of the device. Additionally, once the battery expires after its 3- to 5-year lifespan, another surgery is required to replace the entire control pack. Further complications arise with the wiring that connects the control pack to the probe on top of the skull. It can erode through the skin, again causing infection or necessitating the removal of the entire device. Finally, the patient's

device for turning the implant on and off is a simple magnet which toggles a magnetic reed in the controller. This magnetic reed is susceptible to external magnetic interference, which can cause problems for people around high-power transmission lines, metal detectors, magnetic theft detection systems, and MRI machines.

1.3 PROBLEM STATEMENT

To resolve these issues, a small implantable device capable of controlling and driving a DBS probe is to be designed, built and tested. The device is to be remotely powered, requiring no internal batteries or external connecting wires. The size of the device is to be such that it can be implanted directly under the scalp on top of the skull. These two improvements alone eliminate the need for the relatively large stimulator and subcutaneous wires running through the chest, neck and around the skull as are present on the existing DBS device. In addition, no extra surgery is needed after the initial probe implantation procedure being that the device can be attached to the probe after capping the skull, and no internal batteries exist to ever need replacement. Communication with the device for control and programming is to be accomplished solely via an RF protocol, reducing the more commonly possible magnetic interference with the function of the device. RF interference immunity will be accomplished through encoding that is not likely to be duplicated in a normal ambient environment.

2.0 REQUIREMENTS AND SPECIFICATIONS

This chapter details the technical functions of the device from a structural point of view. Its usage and some design criteria are considered.

2.1 BASIC FUNCTION AND OPERATION

As an implantable DBS device already exists and is being used in patients, the required stimulation profile and range of parameters are fairly well known. Although the currently marketed device has frequency, amplitude, and pulse width ranges of 2-185 Hz, 0-10.5 V, and 60-450 μs, respectively [4], these wide ranges are not fully used. Typically, the pulses administered to the brain are between 60 and 240 μs biphasic waveforms with a frequency of approximately 185 Hz. These pulses range in amplitude from 1.5 V to 3.0 V. However, in normal usage, rarely does the amplitude exceed 2.5 V [5]. See Figure 3 in which each of these three parameters in the pulsing waveform is illustrated. Additionally, the single probe entering the brain has four electrode contact locations to deliver the pulses to the brain. The current device being used is able to administer pulses to two of these electrodes, with the other two acting as ground or neutral terminals. This provides flexibility in tuning the treatment once the probe is implanted. Finally, the pulsing treatment must be able to be turned on and off independent of the actual stimulation profile.

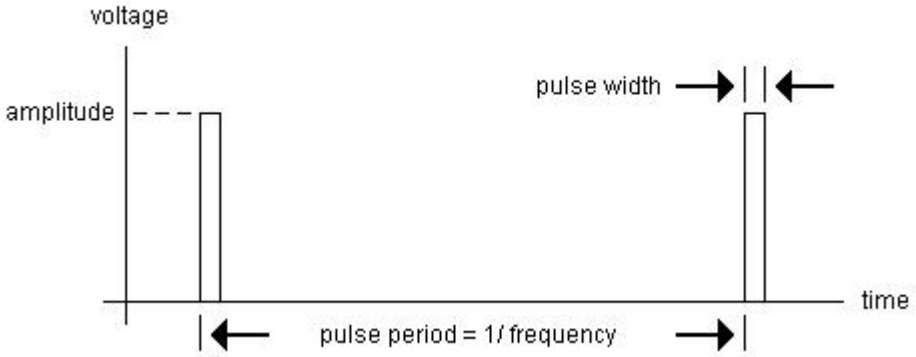

Figure 3: Stimulation pulse profile.

For simplicity in the proof of concept design, some flexibility is sacrificed without any loss to generality. The device constructed for this research adheres to the parameters in Table 1.

Table 1: Developed prototype's pulsing parameters.

Parameter	Range of Values
Pulse Amplitude	2.3 V, 2.7 V, 2.9 V, and 3.0 V
Pulse Width	64 µs, 128 µs, and 192 µs
Pulse Frequency	~190 – 195 Hz
Pulse Location	Four separate locations
Stimulation	On and off

With modifiable parameters comes the need for a remote programming device, or programmer. The programmer must be able to send a recognizable signal to the implanted device via an established communication protocol to modify any of the pulsing parameters. Thus, the implantable device requires a method for receiving and utilizing these signals.

In addition to stimulation and communication requirements, perhaps the most important part of the implantable device is that which receives energy from an external source. This energy is used to power the entire implant and forms the crux of the motivation of this research. A powering scheme using inductive coupling is developed with coils for transmitting and receiving on an external supply and on the implant, respectively. This is the means by which a battery and powering wires are eliminated.

2.2 POWER OPTIMIZATION

Besides simply functionality, the power aspect is an important facet in the design of the DBS device. Minimizing power consumption is generally a worthwhile goal to consider during any design, but it plays a much larger role in the context of remotely powered electronics. Although inductive coupling (the near-field powering technique) can generally provide more energy than far-field powering techniques, future implementations of the implantable device will aim to gather their energy via a far-field powering scheme. This being the case, the device is designed to reduce power consumption wherever possible at the initial design stage in order to provide a simple transition to future prototypes utilizing a far field energy source.

3.0 DESIGN OF THE DEVICE

Chapter 3 details the design decisions for each of the three main parts of the DBS device: the control circuitry, the powering circuitry, and the device programmer.

3.1 CONTROL CIRCUITRY

The main part of the device as a whole is the actual implanted circuitry. This circuitry, which drives the DBS probe, contains a microcontroller and various peripherals for stimulation flexibility and communication. As discussed in Section 2.2, the implant is designed with the key focus of minimizing power while preserving functionality. The circuit's energy usage will be analyzed following the presentation on design.

In order to organize the design process, a general system-level diagram is created. This diagram, shown in Figure 4, outlines the interconnections of the circuitry and helps in pinpointing necessary key elements.

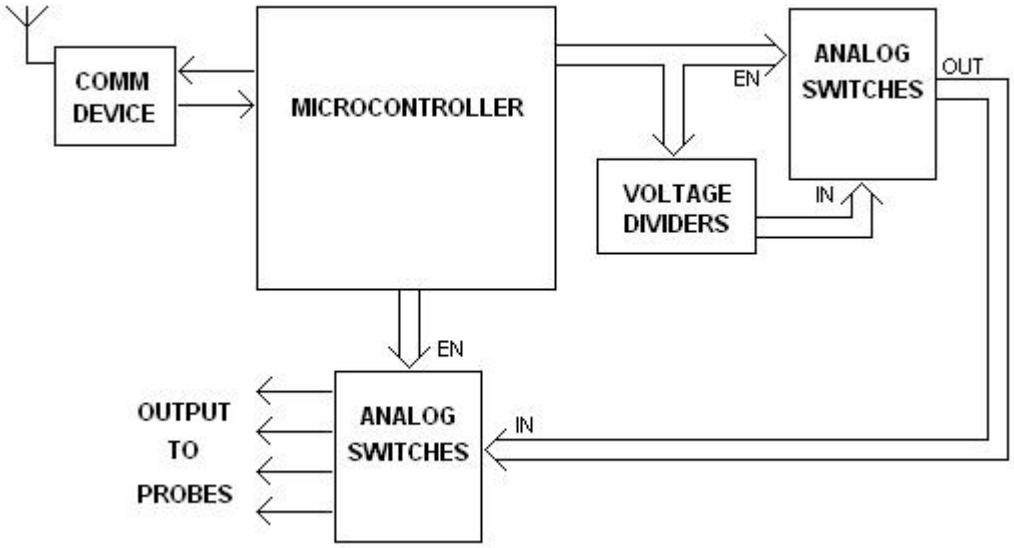

Figure 4: System-level diagram for control circuitry.

As seen in Figure 4, the implantable control circuitry consists of four main elements: a microcontroller, a communication device, voltage divider circuitry and analog switches. The microcontroller outputs the actual pulses, along with the appropriate switch enable signals, which go through any one of the voltage dividers, chooses to which probe conductor the pulses go via one bank of switches, and also listens for programming commands from the communication device. Because of the complexity of the controller function, it will be discussed separately from the peripheral components.

In addition to selecting components, the supply voltage of the circuitry must be evaluated and selected. To save energy, the lowest voltage possible should be chosen, again, while preserving functionality. The highest voltage necessary, as seen in the design parameters of Table 1, is three volts, necessary for the maximum pulse output voltage. This being the case, the supply voltage of three volts is chosen.

3.1.1 Controller Design

The microcontroller chosen for the DBS device, a Microchip PIC16LF87, is the core of the control circuitry. This particular selection was based on a number of factors. First, its two I/O ports afford enough I/O pins to connect to all necessary peripherals. Two pins are used to communicate with the communication device, four pins control the switches before the probe outputs, and the remainder of the pins can be used to select various voltage amplitudes from the array of voltage dividers. Second, the PIC16LF87 has a sleep mode into which it can enter to preserve power when pulsing is not necessary. With this particular chip, the watchdog timer timeout, used as the wakeup mechanism, can be scaled down so that the microcontroller can actually enter sleep mode between pulses produced for the deep brain stimulation. Finally, an external RC oscillator is used with this microcontroller, allowing the high-speed internal oscillator to be turned off for additional power savings.

After the selection of the PIC16LF87, its implementation parameters must be determined. First and foremost is the oscillator frequency. As a lower frequency oscillator uses less power, the lowest frequency that preserves intended functionality should be chosen. Since the most time-critical part of the microcontroller's operation is that of the output pulses, their timing determines the clock speed. Then, because the smallest pulse width in the design criteria is 64 μs and changing an I/O state takes only one instruction cycle, the period of one instruction cycle should be 64 μs, corresponding to an instruction frequency of ~15.6 KHz and thus an oscillator frequency of 62.5 KHz. Practical implementation at this frequency, however, is impossible, thus the frequency must be increased. Doubling the oscillator frequency to 125 KHz gives an instruction cycle time of 32 μs, enabling the creation of 64 μs pulses and proper overall functionality.

The program loop which executes inside the microcontroller is outlined in the flow chart of Figure 5. When powered, the controller initializes the watchdog timeout period and I/O ports, resets the communication chip, sets default pulsing parameters specified by the user at the time of programming, and begins execution of the loop. The "Get / change parameters" stage is discussed in the Section, 3.3.1. The actual pulses created and to which probes they are applied are determined by parameters within the code, one each for amplitude, duration and location. Separate frequency and on/off variables add delay into the pulsing cycle and determine whether pulsing is performed. See Appendix A for the actual microcontroller code.

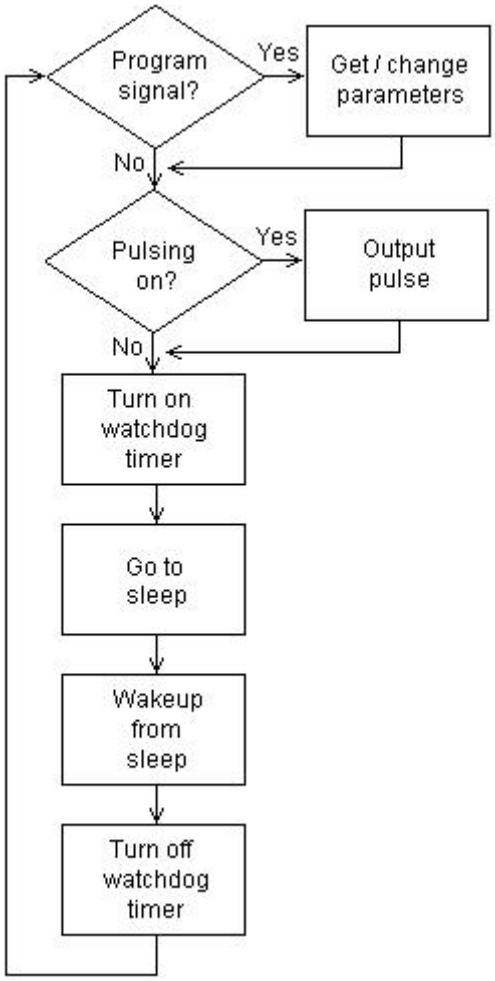

Figure 5: Program execution flow chart.

3.1.2 Peripheral Components

This section details the less complex components of the implant, namely the communication chip, the voltage dividers, and the analog switches.

The receiver chip chosen is the ATA5283 from Atmel. This device was originally intended for tire pressure monitoring applications but is easily adapted for this purpose. It uses a simple ASK protocol at a frequency of 125 KHz. The chip stays in standby mode until it senses a 125 KHz preamble of at least 5.64 ms, after which it wakes up and outputs digital data based on the presence of the 125 KHz signal. After data transmission, a simple digital high input to the reset pin puts the device back to sleep. The antenna used in this application is a small wire wrapped around the circuitry perimeter. A large pull-up resistor of 2.2 MΩ is used on the data output pin to ensure it initializes to a logic high value upon powering of the device.

The amplitude adjustment circuitry is realized by four different voltage dividers providing four different voltage levels, adequate for the proof of concept design. Each voltage divider is driven by a direct pulse from the microcontroller which also closes the switch through which the voltage is applied. Only one of the dividers is pulsed at any one time.

Both switch banks are implemented with Maxim MAX4066A analog switches. These prove convenient due to their small size (four switches on a chip) and ease of use. The first switch bank follows the voltage dividers, each switch enabled by the microcontroller only when necessary. All four outputs are tied together and connected to the four inputs of the second switch bank, which output to the probes. These switches are also enabled by the microcontroller, based on its internal probe output variable.

Figure 6 shows a detailed connection diagram of the control circuitry as a whole.

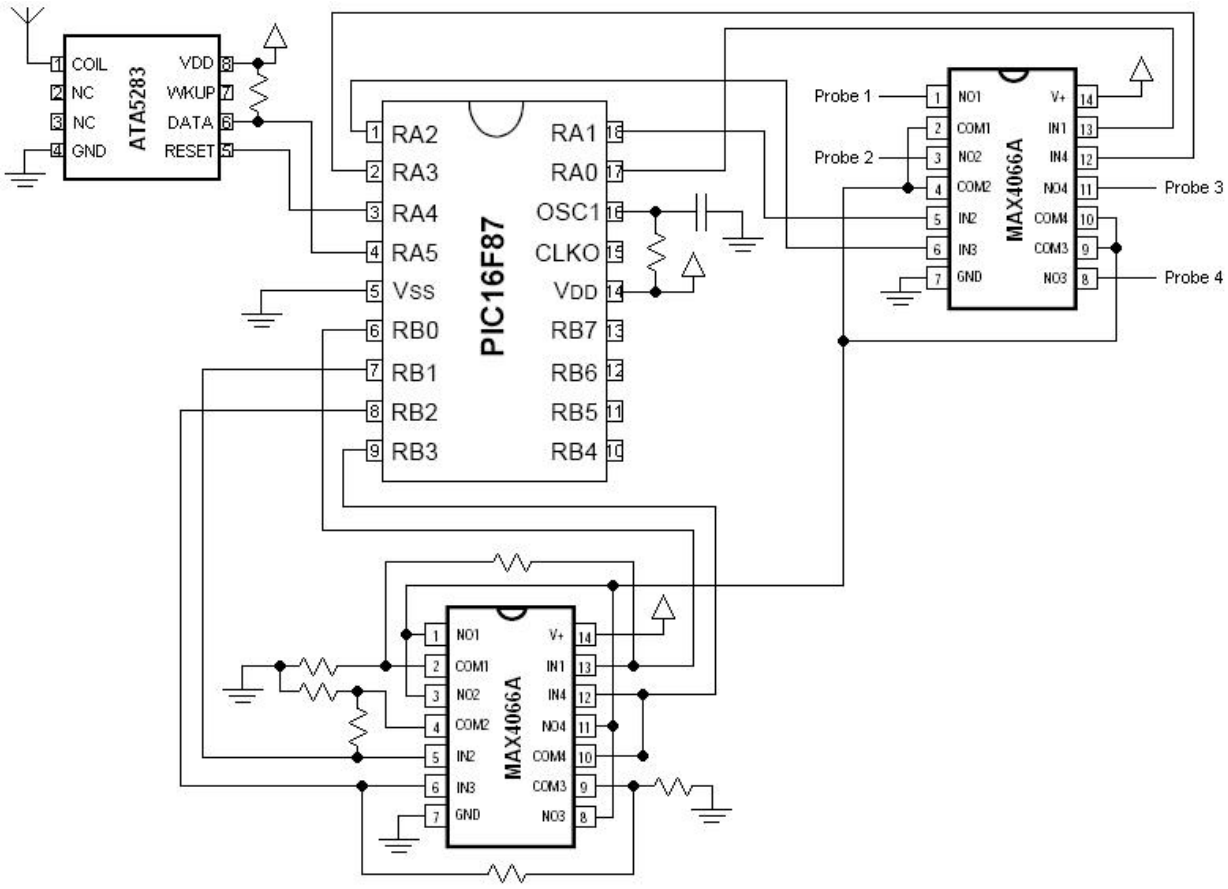

Figure 6: Detailed connection schematic of control circuitry.

3.1.3 Energy Usage: Analytical and Empirical

Given the above detailed circuitry, its estimated power rate and energy usage can be calculated analytically by examining each of the components individually. Conservative calculations are performed with the maximum listed values at room temperature from the respective datasheets. The device is assumed to be pulsing one probe constantly for 24 hours, a full day, with a pulse of 120 μs width, 3 volts amplitude, and 190 Hz frequency. These results are then compared to the actual empirically tested energy usage.

The microcontroller has two different energy usage characteristics corresponding to its two modes of operation, sleep and active modes. While in active mode, all on-chip peripheral components are disabled, adding no additional current to the standard supply current values from the datasheet. However, supply current values in the external RC oscillator setup at three volts are only given for frequencies of 1 MHz and 4 MHz: 170 μA and 600 μA, respectively [6]. Assuming a fairly linear frequency dependency, an equation for supply current can be found from these values and the estimated current at 125 KHz extrapolated.

$$I_{DD} = 0.000143 f + 26.66$$

Equation 1: Microcontroller supply current as a function of external RC oscillator frequency.

Using Equation 1, the active mode supply current at 125 KHz is calculated to be 44.583 μA. In sleep mode, four milliseconds of every cycle, the watchdog timer is enabled, adding its required current to the standard supply current in power down mode. From the datasheet, this sum is 5.1 μA [6]. From the active and sleep mode values, the average supply current over one pulsing cycle is calculated to be 14.576 μA, which at the supply voltage of 3 volts gives a power

usage of 43.728 μW. With 86,400 seconds in one day, the maximum theoretical energy used by the microcontroller per day is 3.778 joules.

The Atmel ATA5283 receiver chip remains in sleep mode almost 100% of the time. In any one day it might exit standby mode for a total of one second, as each programming routine takes less than 50 ms. This active mode time is negligible in calculating daily energy usage so only the standby mode supply current will be used. In standby mode, the maximum supply current is 1.5 μA [7], corresponding to 4.5 μW at 3 volts. At this power rate, the energy used per day is 0.389 joules.

The MAX4066A chips use a maximum of 1 μA quiescent current each [8]. With two switch banks, this becomes 2 μA total, or 6 μW at 3 volts. In one day, this equates to an energy usage of 0.5184 joules.

The voltage dividers only use power during actual pulses. However, their resistances are large compared to that of the tissue resistance in parallel, thus the equivalent resistance seen by each output pulse is approximately that of the tissue. This being the case, the daily energy usage of the output pulses can be calculated by examining the energy dissipated in the tissue alone. Using a model tissue resistance of 10 KΩ [9], the power dissipated during a pulse is $(3 \text{ votls})^2/10$ KΩ, or 0.9 mW. With a frequency of 190 Hz and constant pulsing, 16,416,000 pulses occur per day. With each pulse being 120 μs, the actual total pulse time is thus1969.92 seconds per day, corresponding to 1.77 joules per day.

Finally, the energy usage of the voltage regulator in the powering circuitry, described in the next section, must be taken into account. From the datasheet for the LT1521-3, the maximum ground pin current is 20 μA [10], corresponding to 60 μw at 3 volts. Powering for a whole day, 86,400 seconds, it uses a total of 5.184 joules.

The maximum theoretical energy used per day is simply the sum of all individual components' energy usage, a total of approximately 11.64 joules per day.

Empirical tests were performed to find actual energy usage characteristics of the circuitry. These results have been compared to theoretical calculations. The tests were performed by powering the circuitry with a power supply and measuring the voltage across a small resistor in series with the circuitry to find the average supply current. The power follows from the current and supply voltage product, which is used to find total energy usage per day.

The series resistor is measured while disconnected from the circuit, having a value of 1.05 Ω. The power supply is then set to 3 volts and connected to the input of the voltage regulator. The average voltage across the resistor is measured to be 42 μV, corresponding to an average supply current of 40 μA. With a circuit supply voltage of 3 volts, the power is calculated to be 120 μW, for a total energy usage of 10.37 joules per day.

The above test is repeated with a power supply voltage of 5 volts. The average voltage across the resistor is 44 μV, corresponding to 41.9 μA, slightly higher in this case due to more power dissipation in the voltage regulator. The supply voltage of three volts is still used, for a power of 125.7 μW and total energy usage of 10.86 joules per day.

The actual energy usage approaches the theoretical maximum, within approximately one joule per day. Various uncalculated losses in the circuit such as leakage current and non-ideal timing in the microcontroller account for the high power requirement, as does the relatively inefficient voltage regulator.

3.2 POWERING CIRCUITRY

Once the control circuitry is designed, the powering circuitry simply needs to supply enough power to make it operative. The challenge in this design is in making the remote powering circuitry small enough both on the implant side and externally, so that both will be inconspicuous in the final prototype. Because the intended powering scheme is the wearing of a hat or cap to hold the external powering circuitry, said circuitry will be relatively close to the actual implant, allowing for the usage of near-field inductive coupling of the external and internal circuits. Because of losses in the coupling, a voltage boosting circuit is required on the internal circuitry to reach the desired supply voltage. Finally, a voltage regulator must be used to prevent spikes in the supply voltage or overdrive of the control circuitry.

The circuitry is developed in two stages, the first of which is the implementation of the voltage boosting technique. Knowing that the inductive coupling will provide an alternating current and that a DC voltage output is required, the circuitry must be able to amplify and rectify a signal. The obvious choice is to use a charge pump, sometimes referred to as a voltage doubler or multiplier. See Appendix C for a detailed description of charge pump functionality. Basically, one stage of a charge pump doubles the amplitude of an AC input voltage, storing the doubled DC voltage on an output capacitor. Successive stages essentially double the voltage from the previous stage. Assuming the inductive coupling will be able to provide at least 0.5 volt, three stages should be able to provide a 4-volt DC output, enough to drive the control circuitry. A 3-stage charge pump was constructed on a circuit breadboard to experiment with and test the circuit design. In experimenting with the charge pump, square waveforms with 50% duty cycle were found to produce a higher voltage output than other waveforms, such as triangular, sinusoidal, or non-50% duty cycle square waves.

The second stage of design is that of implementing the inductive coupling technique. In developing the actual circuitry, prototype PCBs were created with variously sized coils for testing. See Figure 7 and Figure 8.

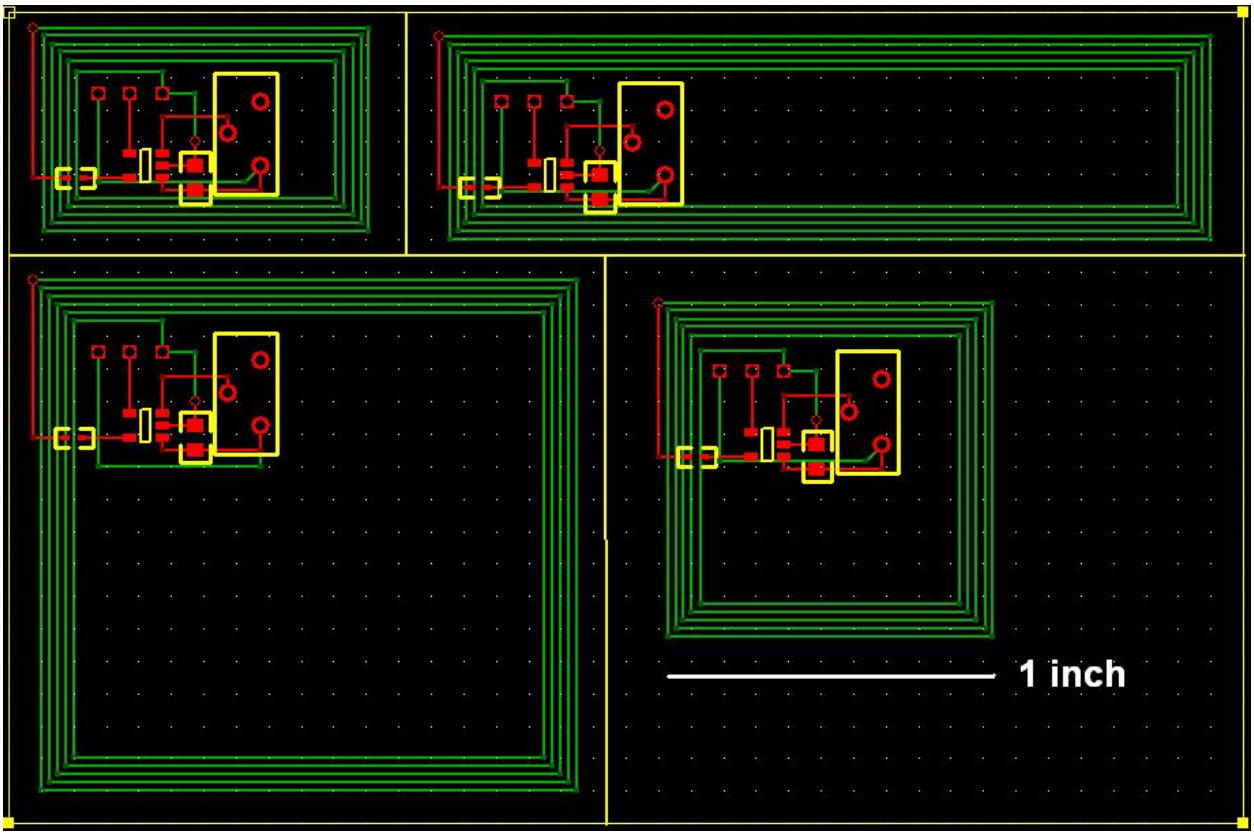

Figure 7: Transmission boards for inductive coupling testing.

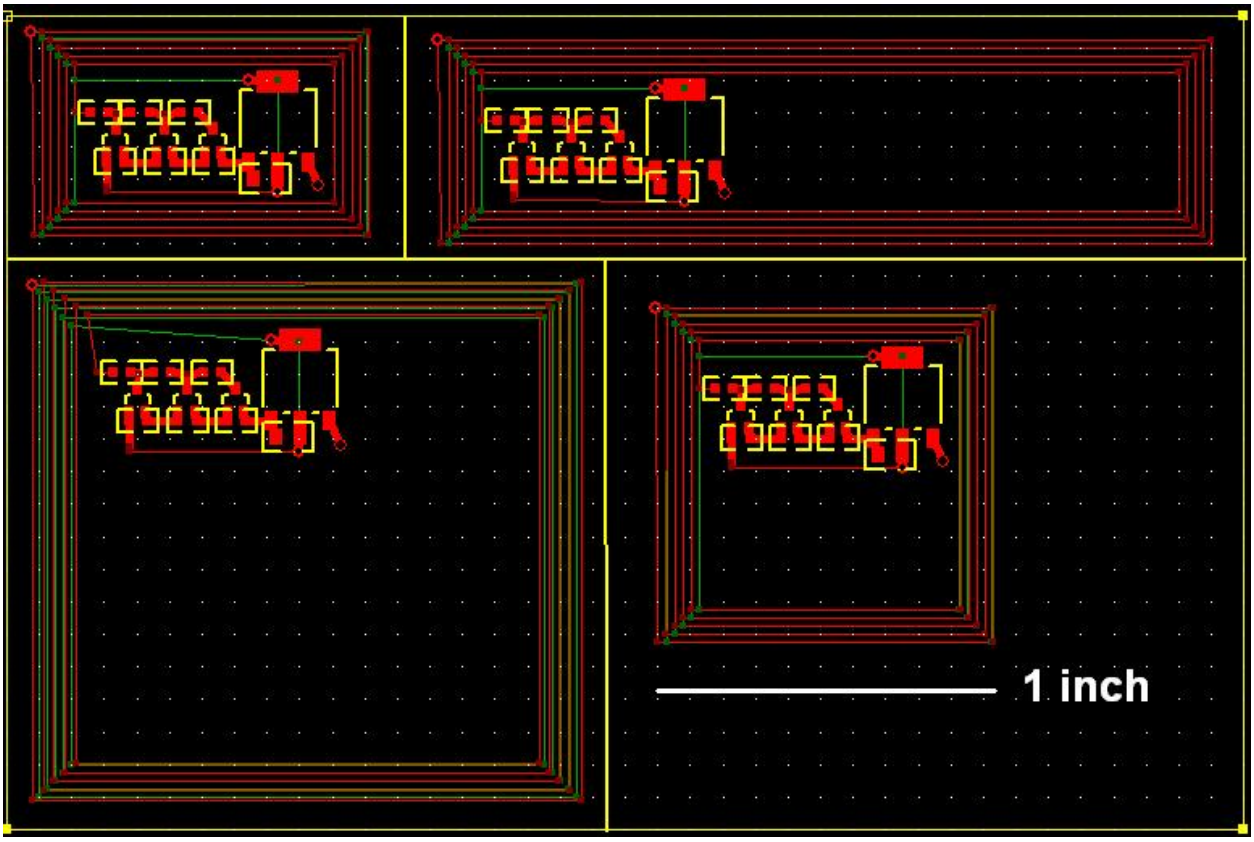

Figure 8: Receiving boards for inductive coupling testing.

The transmitting coil PCBs contain pads for an adjustable oscillator, the LTC6900, and 200-KΩ potentiometer, along with the coil windings. The LTC6900 creates a 50% duty cycle square wave at frequencies between 1 KHz and 20 MHz. Pads for a surface mount resistor in series with the coil are also included. The receiving coil boards contain pads for charge pump components, 1-µF capacitors and BAT54SW-7 diodes, as well as a small profile 3-volt regulator, the LT1521-3. Figure 9 details the connections.

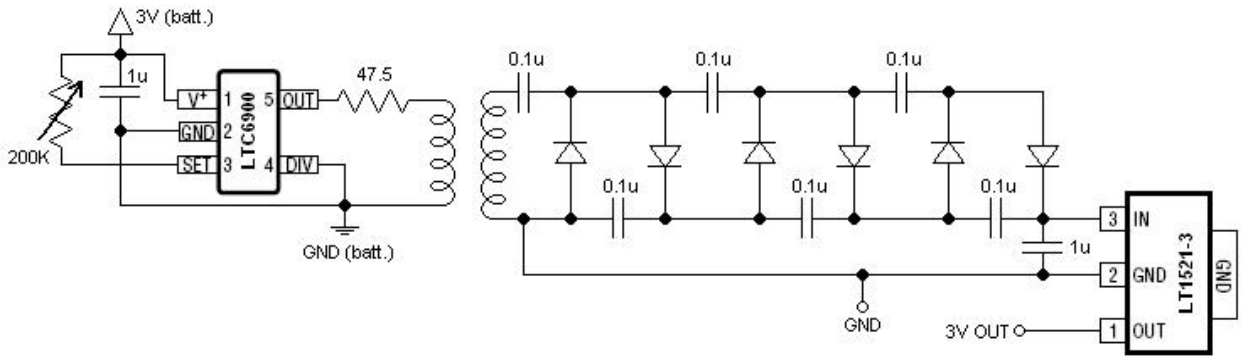

Figure 9: Powering circuitry schematic showing detailed connections.

After soldering all components on the boards, each pair of transmitting/receiving boards was tested. Note the transmitting board coil has five turns while the receiving board coil has ten turns, for a turns-ratio of 1:2. The transmit boards were powered with 3 volts from a power supply and the oscillator frequency adjusted to determine the maximum regulator output voltage on the receiving boards. Using multiple different resistance values for the transmit coil series resistor, a 47.5 Ω resistor was found to produce better results than other available resistances, so only those tests are included in the current discussion.

Both the 6 cm x 1.6 cm couple and the 4.3 cm x 4.1 cm couple produced no output voltage at any distance. The 2.5 cm x 1.5 cm boards produced a maximum output voltage of 1.47 volts when they were less than 1 mm apart. This voltage persisted with increasing distance to 7 mm, and then the voltage dropped off. The 2.6 cm x 2.6 cm boards, arguably the best performing, produced an output voltage of 3 volts, the regulator maximum. This voltage persisted up to 12 mm of separation. Thus, this latter board configuration was decided upon to be used for means of powering the prototype. The transmitting oscillator frequency was varied between 2 MHz and 15 MHz depending upon the distance between the coils and the dielectric

between them. Frequencies around 14 MHz generally produce adequate power transfer in most cases.

In investigating the inductive coupling design to find ways to decrease overall power consumption, the input voltage to the regulator was measured to be 7-8 volts. Hence, some power is wasted in the voltage regulator. A smaller turns-ratio could thus be used to supply less voltage and more current, optimizing power usage. Five of the ten turns in the receiver coil were shorted, reducing the turns-ratio to 1:1. This setup was still able to supply the necessary 3-volt output voltage with the input to the voltage regulator reduced to 3-4 volts, decreasing power dissipation in the regulator and increasing overall power efficiency.

With the design of the powering circuitry complete, the circuitry must be integrated with the control circuitry. Figure 10 shows the relative layout of the circuitry combination.

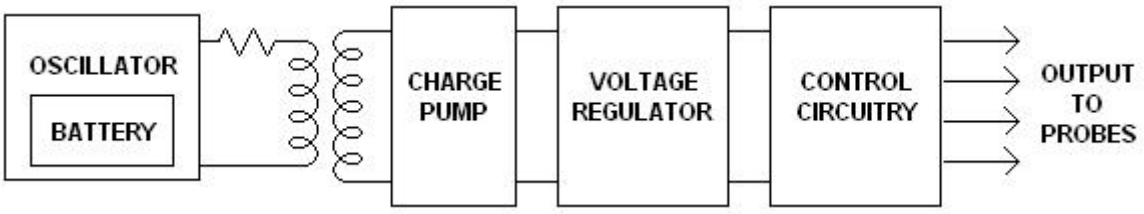

Figure 10: Integration of powering scheme and control circuitry.

A PCB was designed combining both the powering and control circuits as shown in Figure 11. The top side of the board, red and yellow, contains the control circuitry, while the underside of the board, green, contains the coupling coils and powering circuitry. Again, a small wire was attached to the coil input of the ATA5283 and placed around the perimeter of the board as the prototype of the programming antenna.

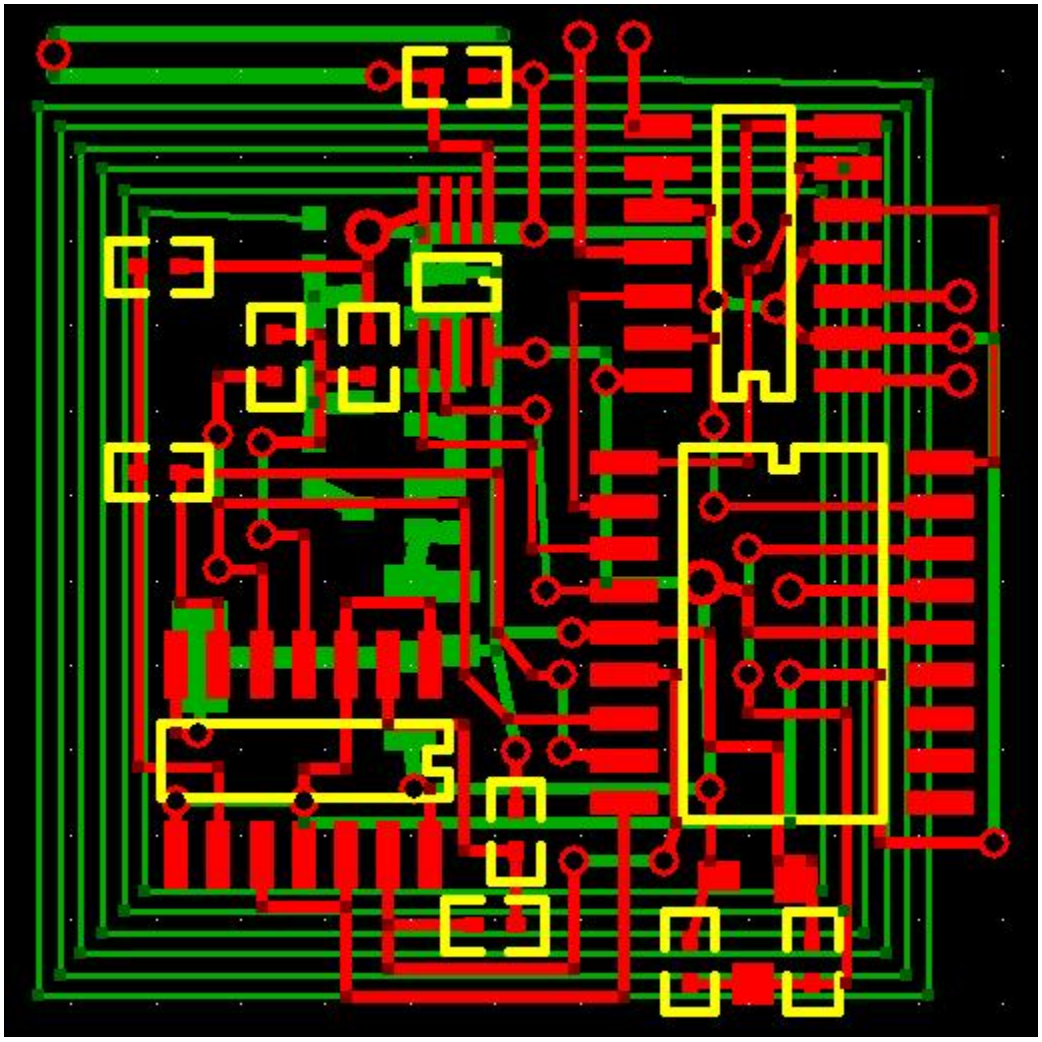

Figure 11: Final prototype PCB combining power and control circuitry.

Implementations of the final prototype, external powering and internal implant, can be seen in Figure 12 and Figure 13, respectively.

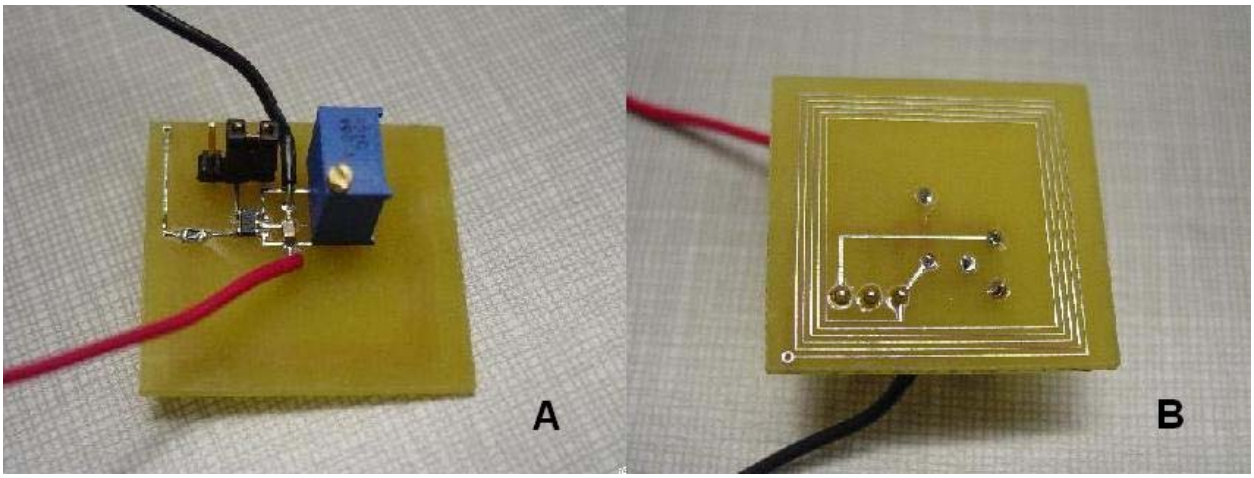

Figure 12: External powering oscillator coil. (a) Top. (b) Bottom.

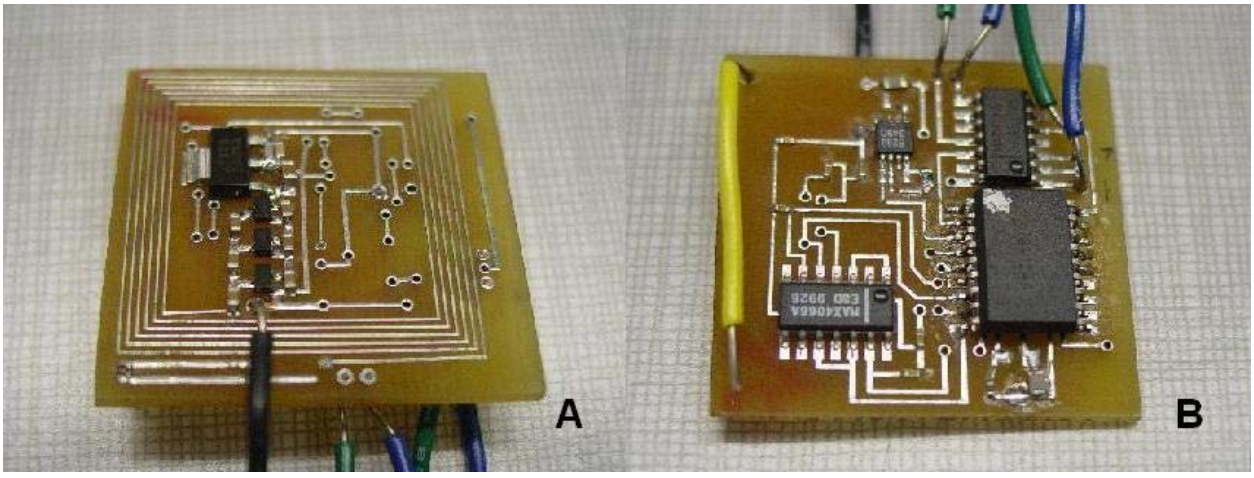

Figure 13: Control and powering implant circuitry. (a) Top. (b) Bottom.

3.3 PROGRAMMING DEVICE AND PROTOCOL

The final necessary component required to complete the functional device is the external programmer. The programmer needs to be able to communicate successfully to the control circuitry in order to change the pulsing parameters after implantation. As discussed in Section 3.1, the control circuitry includes a LF receiver chip sensitive to 125 KHz ASK signals. Thus, the programmer must be able to produce such a signal, and a protocol must be established for coherent communication.

3.3.1 Communication Protocol

The transmission signal of the protocol is implemented in five blocks: wake-up, start gap, header, type, and value. The wake-up signal, or preamble, is required by the ATA5283 chip to be at least 5.64 milliseconds of a constant 125 KHz signal. The 125 KHz signal is held for 8 milliseconds by the programmer to be certain the chip recognizes it. Following the wake-up is a start gap during which no signal is transmitted. This sets the output of the receiver chip to logic low to alert the microcontroller that a communication is going to be sent by the programmer. Because the microcontroller execution loop is approximately 5.4 milliseconds, the start gap lasts for 8 milliseconds, allowing enough time for the microcontroller to recognize the low input no matter where it is in program execution when transmission starts. Once the microcontroller is aware of and ready for transmission, the actual programming instructions can be sent. Each bit of this "frame" is sent via a 125 KHz ASK protocol in which each bit lasts 2 milliseconds, enough time to allow for the microcontroller's slower operation to keep up. First is the header, consisting of the sequence 1010. If the microcontroller does not see this exact sequence, it abandons the programming routine, waiting 30 milliseconds before resetting the receiver chip. If

the header is received correctly, the microcontroller then checks the next seven bit intervals, storing the first three bits as a "type" variable and the next four bits as a "value" variable. After transmission, the microcontroller resets the receiver chip, putting it into its standby-listen mode. The microcontroller then determines which pulsing parameter to change based on the "type" variable and decodes the "value" variable into the appropriate change for that parameter. Table 2 shows the bit codes for each parameter. The microcontroller then resumes the regular program execution loop. See Appendices A and B for the microcontroller and programmer codes respectively.

Table 2: Bit codes for "type" parameter in communication protocol.

Parameter	"Type" Bit Code
Pulse Location	000
Pulse Amplitude	001
Pulse Duration	010
Pulse Frequency	011
Stimulation On/Off	100

3.3.2 Programming Device Design

The programmer requires two main components: a method for letting the user select what data to send and the actual means to transmit the data. A microcontroller is used to interpret the slide switch inputs and control the output signal. The PIC16F87 is chosen for this purpose due to the designer's familiarity with the chip and its suitability for this purpose. Four slide switches on the

programmer set the "value" parameter and five different switches are available for setting the "type," or which pulsing parameter to change. Only one of these five switches should be on at any one time. A single button press initiates the communication, upon which the microcontroller reads the states of the switch inputs then outputs the corresponding signal according to the protocol discussed in Section 3.3.1. However, the microcontroller can not create a healthy sinusoid for transmission by itself, so instead it sends pulses to a MOSFET driver, the TC4422, which in turn drives an LC circuit tuned to 125 KHz. See Appendix D for calculation of the inductor and capacitor values. The TC4422 is powered directly from a 12-volt, 30-watt power supply so as to provide enough current to drive the high voltage and current oscillations in the resonant circuit. Figure 14 shows the PCB layout for the programmer while Figure 15 shows the detailed connections schematic.

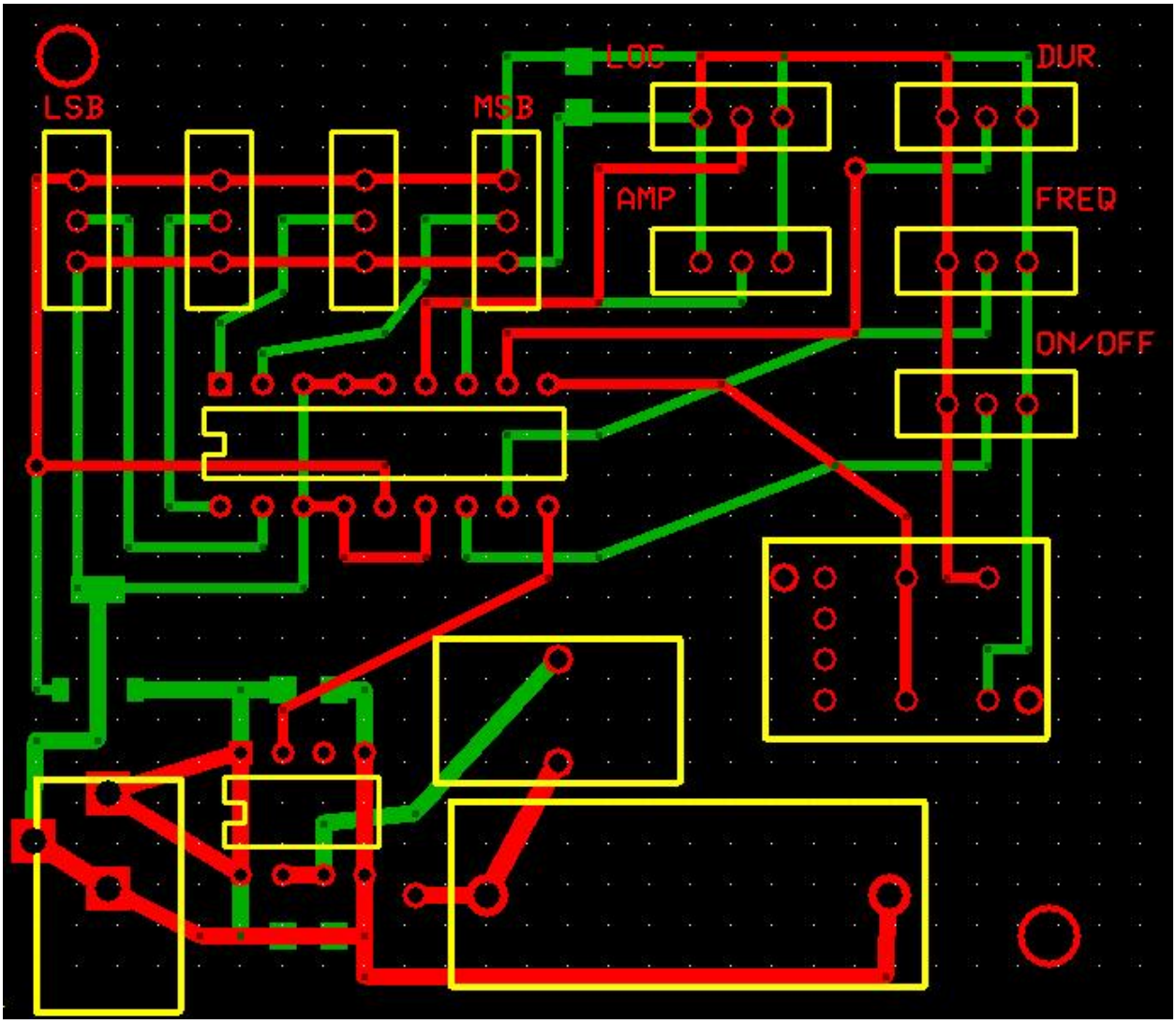

Figure 14: Programmer PCB layout.

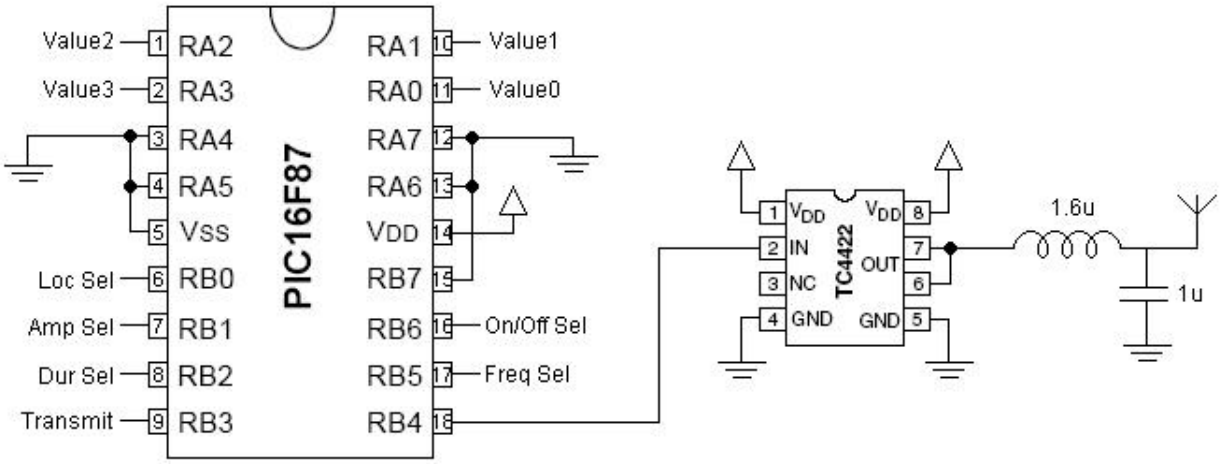

Figure 15: Detailed connections schematic of the programming circuitry.

The resonant circuit alone is not enough to send a strong signal to the control circuitry. It requires an antenna to transmit the 125 KHz signal more efficiently. For this purpose, a PhidgetRFID antenna, designed for use with 125 KHz RFID systems, is used. A simple solder joint connecting one end of the antenna to the capacitor proves functional.

To make the programmer easy to handle and use, a small handheld box was modified to house the circuitry, with the switches and button available on top and the antenna underneath. Figure 16 shows the CAD model for the modified case and how the different components are put together.

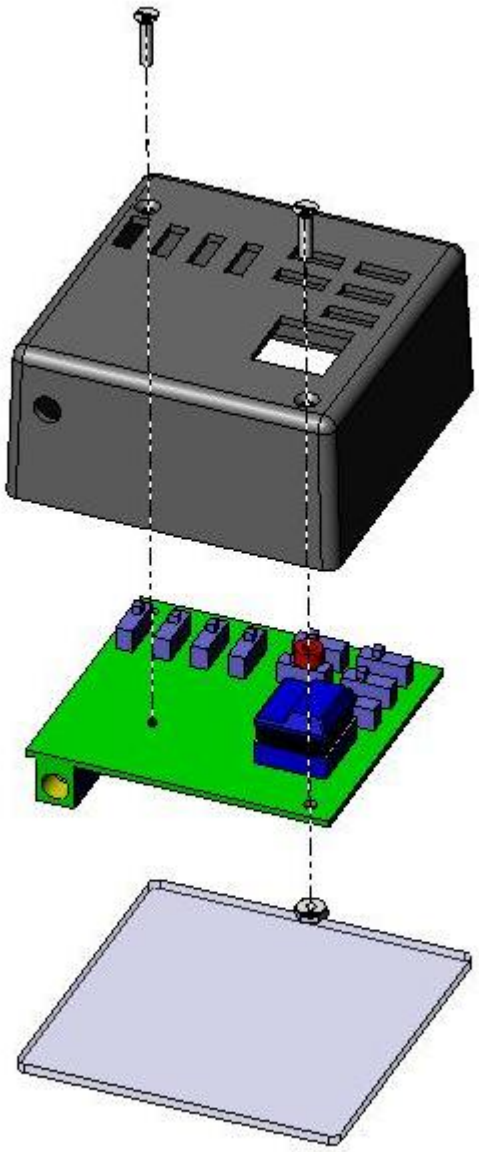

Figure 16: Assembly of the programming device in CAD software.

Figure 17 illustrates the fully assembled programmer, a top view with switches and labels and a bottom view of the PhidgetRFID antenna.

Figure 17: Top and bottom views of the programming device, showing programming switches and button, and PhidgetRFID antenna, respectively.

4.0 PROOF OF CONCEPT EXPERIMENTS

Once the design of the device was finished, testing to ensure its functionality was necessary. This chapter details the testing procedures and methods used to prove the functionality of the implant.

4.1 TESTING THROUGH AIR

Before testing with any intervening material, the power transfer and programmability of the device were tested through air. This guarantees the device is at least functional on its own before any dielectric is added between the external and internal circuitry. Additionally, the actual mechanism of powering was proven to be the inductive coupling of the transmitting and receiving coils.

4.1.1 Functionality and Programming

To test functionality, the external transmitting coil PCB and the internal receiving coil PCB were located parallel to one another at three different distances, 5-, 7-, and 10 mm, corresponding to the average range and extreme values of human scalp thickness [5]. This setup is shown in Figure 18. The transmitting coil oscillator was connected to a power supply initially set to 5 volts. The frequency of oscillation was adjusted to produce a maximum output voltage on the receiving coil circuitry's voltage regulator. At this point, the programming device was tested by placing it behind the top of the transmitting coil PCB and attempting to program all possible

changes to all five pulsing parameters. The pulse output locations of the control circuitry were monitored to verify successful programming. After testing the programming scheme, the supply voltage of the transmitting coil oscillator was lowered in 0.1-volt decrements. At each stage, the maximum output voltage available from the receiving coil voltage regulator was measured and recorded. The resulting data of input vs. output voltage was plotted to compare the efficacy of the design at each distance.

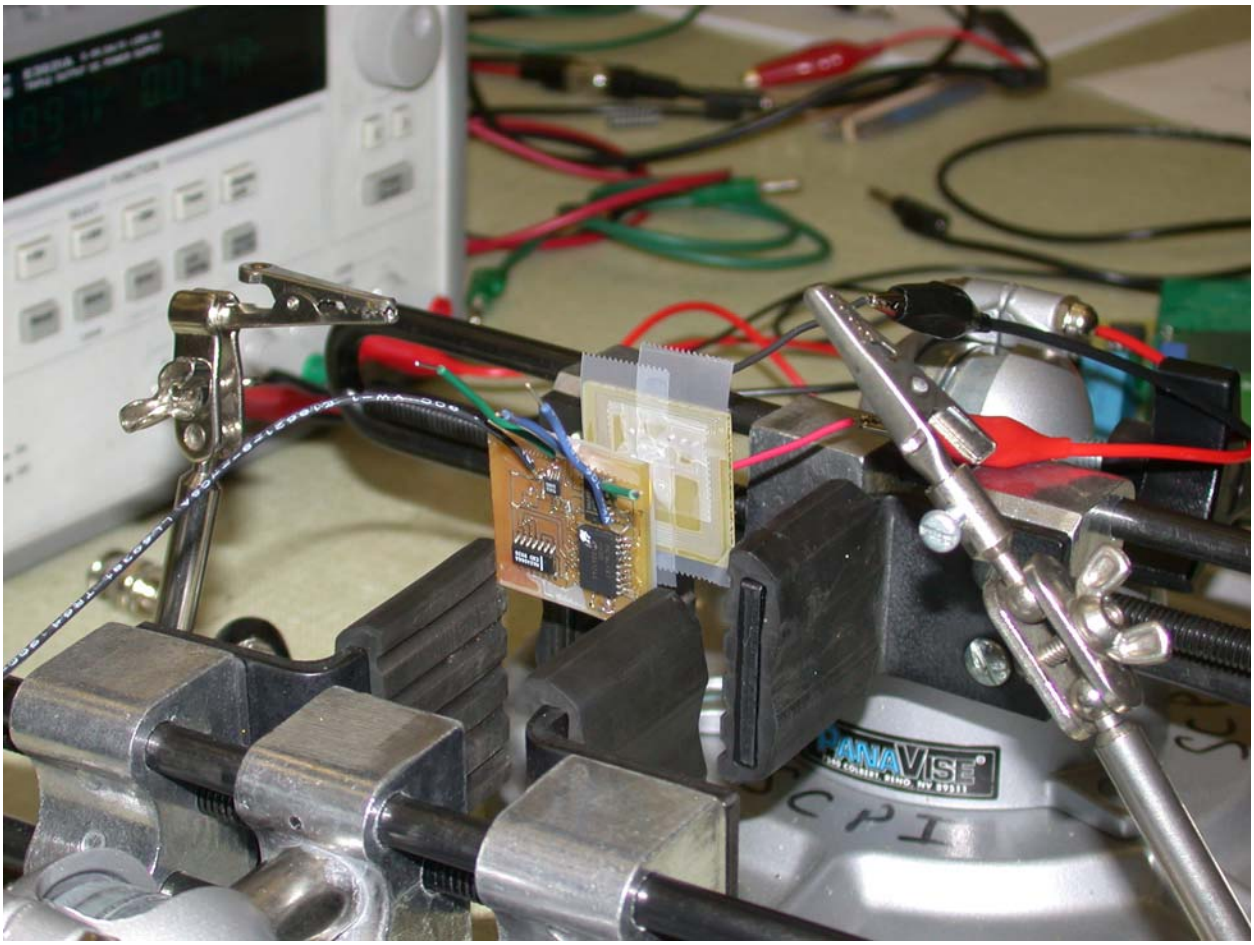

Figure 18: Experimental setup for testing power transfer and programming through air.

4.1.2 Powering Mechanism

To prove that the coils on each of the transmitting and receiving PCBs are indeed the mechanism of power transfer, instead of any of the connecting measurement wires, a simple test was performed. After verifying in a test setup that a powering mechanism exists, the coil on the receiving PCB was cut and the same setup was used to test the powering again. The cut coil can be seen in the top left of Figure 19 and compared to Figure 11. Note the receiver antenna is simply attached to the opposite side of the board and a wire for monitoring regulator output voltage was added.

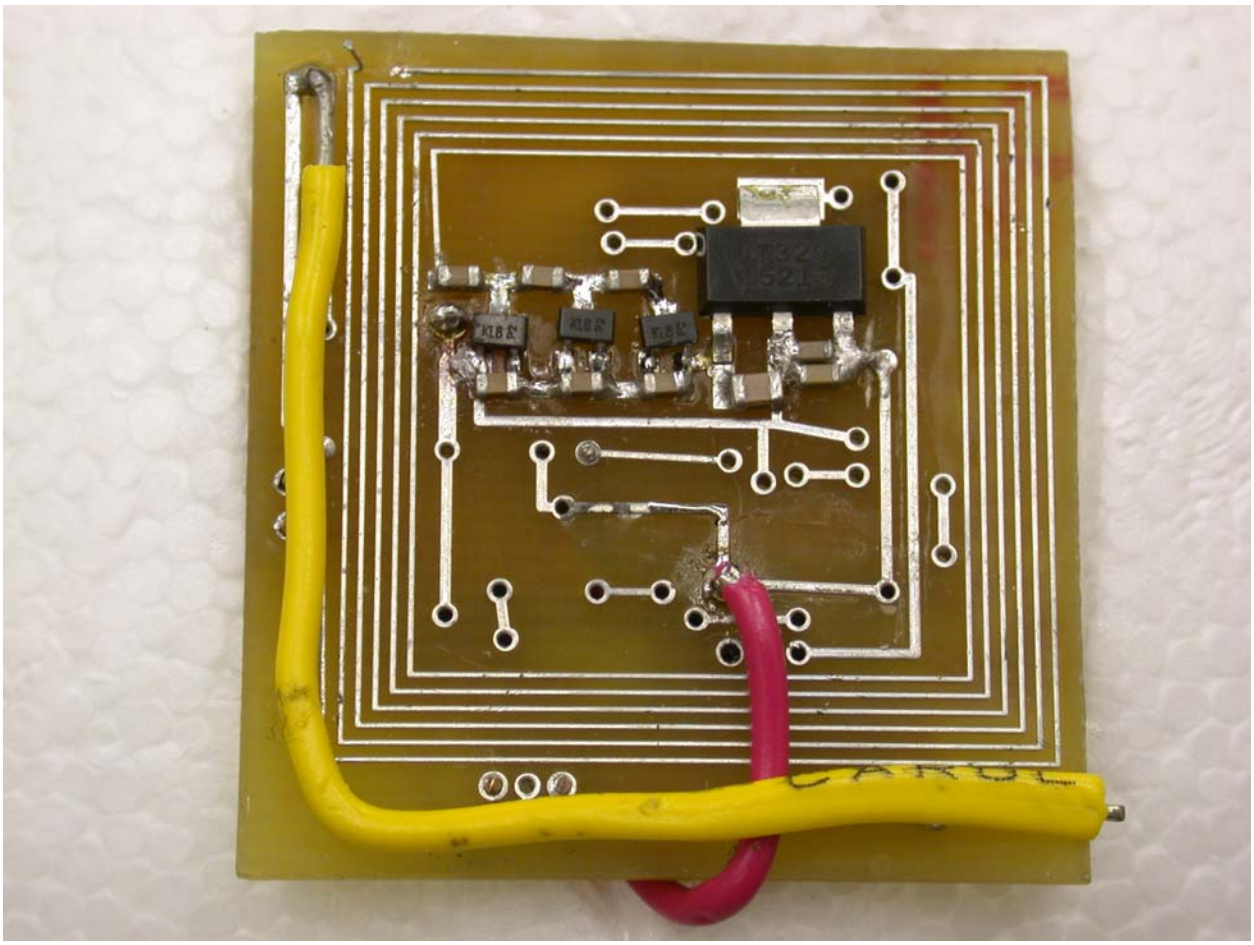

Figure 19: Cut coil to prove powering mechanism.

4.2 TESTING THROUGH SWINE SKIN

After verifying functionality through air, tests were performed with a model scalp layer between the internal and external PCBs. Freshly slaughtered swine skin was used for this purpose due to availability and similarity to human skin. Three different thicknesses were tested: 5-, 7-, and 10 mm, those of the average range of scalp thickness and an extreme maximum [5]. Though the dermis and epidermis of the 7- and 10-mm skins are slightly thicker than those of the 5-mm skin, some extra thickness is due to a thin layer of fat. This should not have a tremendous effect on the reliability of the tests. The transmitting and receiving PCBs were again held in parallel, simply on either side of a piece of skin. Each piece of skin was at least 12-cm square, ensuring all fields associated with the inductive coupling must pass through the skin. To prevent any fluid from the skin interfering with the circuitry, clear tape was put over each side of the PCBs adjacent to the skin. The tape has negligible effect on the inductive coupling. The procedure outlined in Section 4.1.1 was repeated in full. Figure 20 shows the test setup with the 5-mm piece of swine skin.

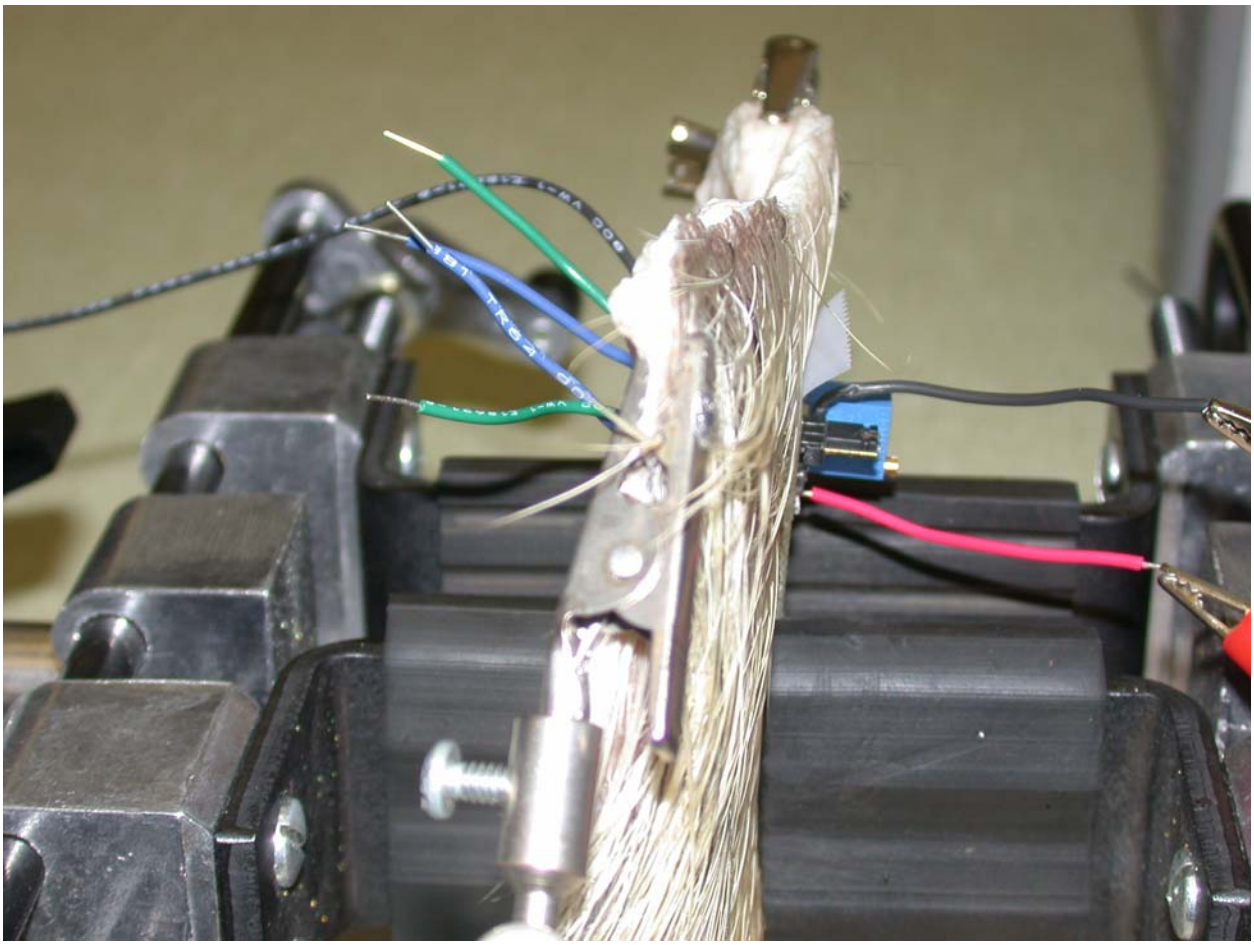

Figure 20: Swine skin test setup with 5-mm thick skin being tested.

While testing the 10-mm piece of skin, after having tested the 5- and 7-mm pieces, the experiment was interrupted, precluding any legitimate data from fresh 10-mm swine skin. All three pieces of skin were then frozen, to be thawed and tested again approximately one week later. The same experimental procedure was repeated for the thawed skin, successful data being gathered for all three thicknesses of skin.

4.3 TESTING THROUGH CADAVER SCALP

To complete the proof of concept, one final test was performed through the scalp of an actual human head. A second prototype was created and encapsulated with an electrical sealant similar to caulking. The sealing was performed to prevent any physical interaction between the circuitry and scalp/skull after implantation. Before sealing, wires were attached to the voltage regulator output, ground reference and the four probe output locations for a means to measure device operation. The same test was performed on this sealed device through air as was performed with the previous prototype in Section 4.1.1. This was done in order to have a reference against which to compare the cadaver scalp tests. The sealed device was then surgically implanted under the scalp of a cadaver head and the external powering circuitry was put into place over the implant. See Figure 21 and Figure 22.

Figure 21: Placement of the implant under the cadaver scalp.

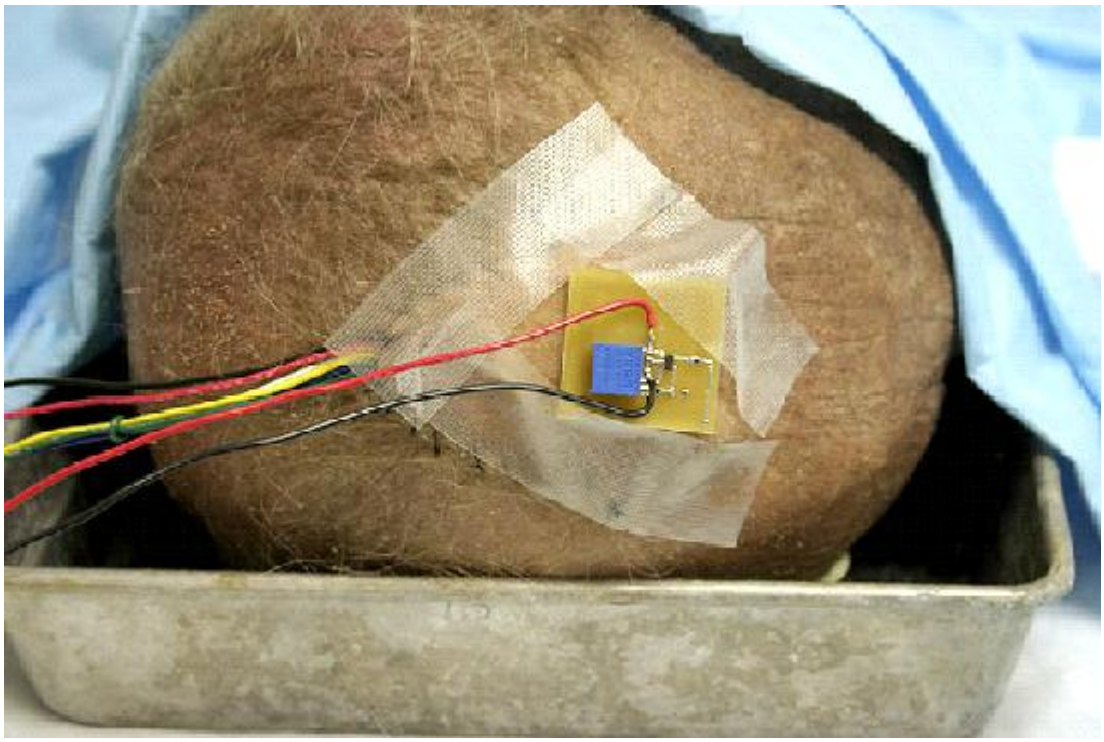

Figure 22: External powering circuitry placed over the implant.

Once the device was implanted and powered, testing commenced similar to that of Sections 4.1.1 and 4.2. The transmitting coil oscillator was attached to a power supply set to 5 volts and the output of the control circuitry voltage regulator was monitored, along with the four pulse output locations. The frequency of the oscillator was adjusted to produce maximum output voltage from the regulator and testing of the programmer commenced. All five pulsing parameters were modified to all possible settings using the programmer, after which the supply voltage to the oscillator was lowered in decrements of 0.1 volt. The maximum regulator output voltage was measured at each of these voltage steps and the results were plotted.

The second experiment involves measuring the regulator output voltage attained at various distances between the external powering coil and the scalp. The supply voltage to the transmitting coil oscillator was set to 4.5 volts to simulate powering by three standard AAA batteries in series. Then, a ruler was placed against the scalp as shown in Figure 23, and the transmitting coil PCB was moved away from the scalp, then towards the scalp, then to random distances from the scalp. The regulator output voltage was recorded at numerous steps along this path and the results were plotted.

Figure 23: Measurement of distance between transmitting coil and scalp.

One final test of a powering hat prototype was performed. The model hat is discussed in Chapter 7.0.

5.0 EXPERIMENTAL RESULTS

This chapter presents the results obtained from the experiments described in Chapter 4.0.

5.1 RESULTS FROM TESTING THROUGH AIR

5.1.1 Powering and Programming

At the oscillator supply voltage of 5 volts, all available parameters were programmed successfully. Figure 24 shows the graph of maximum regulator output voltage against oscillator supply voltage.

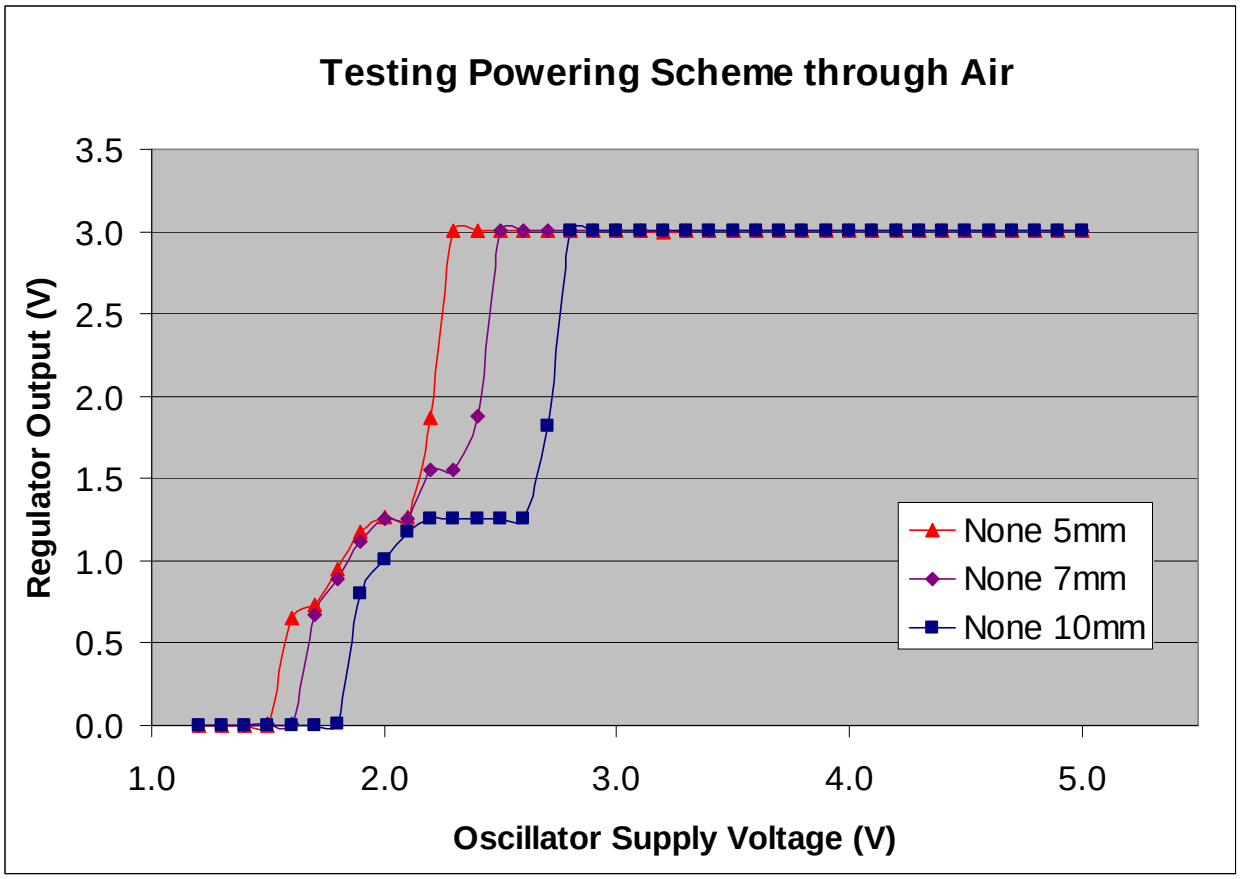

Figure 24: Plot of maximum regulator output voltage vs. oscillator voltage within air.

5.1.2 Powering Mechanism

Shown here are the results of the coil powering experiment. Figure 25 shows the actual test with the oscilloscope voltage in the background, before and after cutting the receiver coil (see Figure 19). Figure 26 shows a close-up of each of the regulator output voltages, before and after cutting the receiver coil. Note the 3.00-volt output before cutting the coil and 13-millivolt output after.

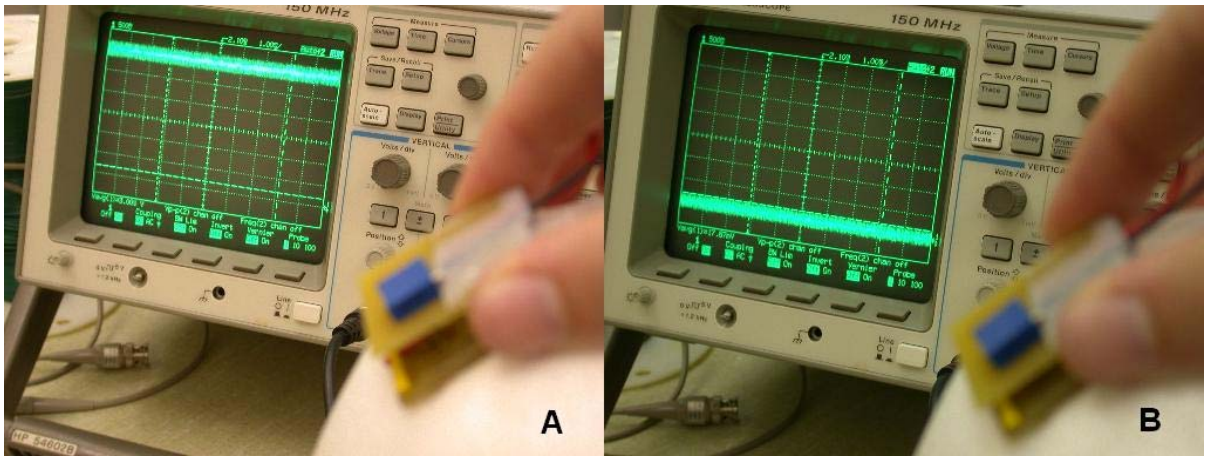

Figure 25: Power mechanism testing (a) before and (b) after cutting the receiver coil.

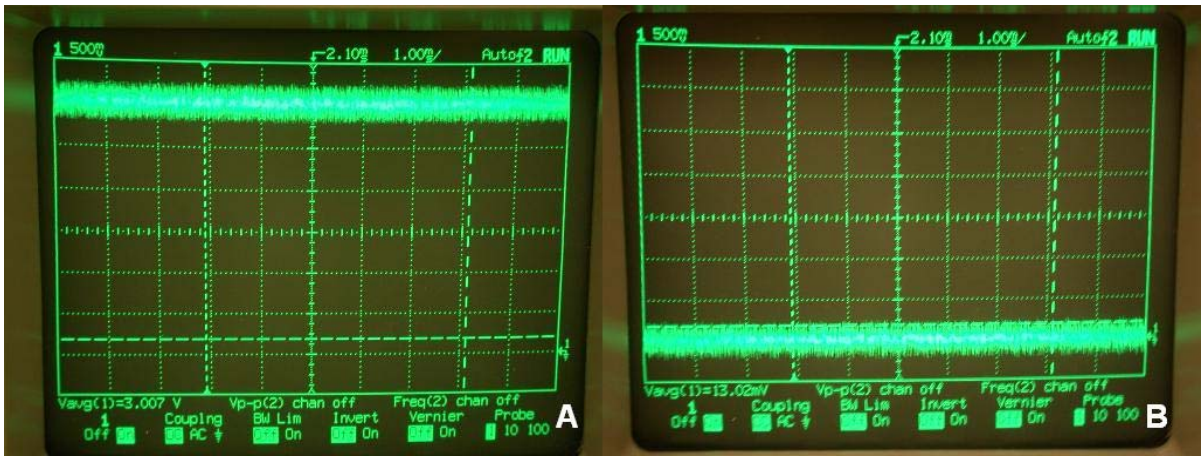

Figure 26: Close-up look at regulator output voltage (a) before and (b) after cutting the receiver coil.

5.2 SWINE SKIN TESTING RESULTS

The programmer successfully changed all variable pulsing parameters through both the fresh and thawed swine skin. Figure 27 shows the graph of maximum regulator output voltage against oscillator supply voltage through fresh swine skin. Also displayed on the graph for comparison purposes are the results from the prototype test through air.

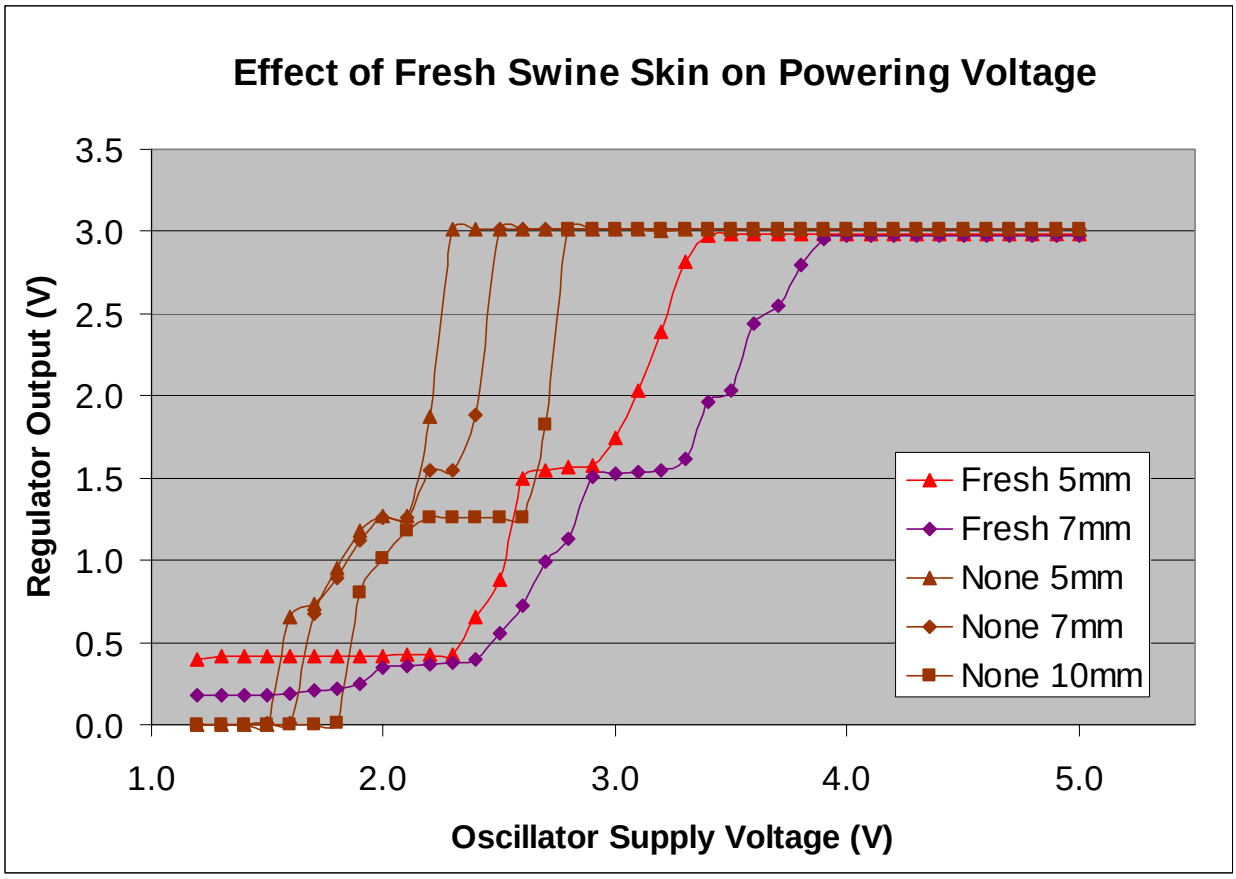

Figure 27: Plot of maximum regulator output voltage vs. oscillator voltage using fresh swine skin.

Figure 28 shows the graph of maximum regulator output voltage against oscillator supply voltage through thawed swine skin. Also displayed on the graph for comparison purposes are the results from testing through fresh swine skin.

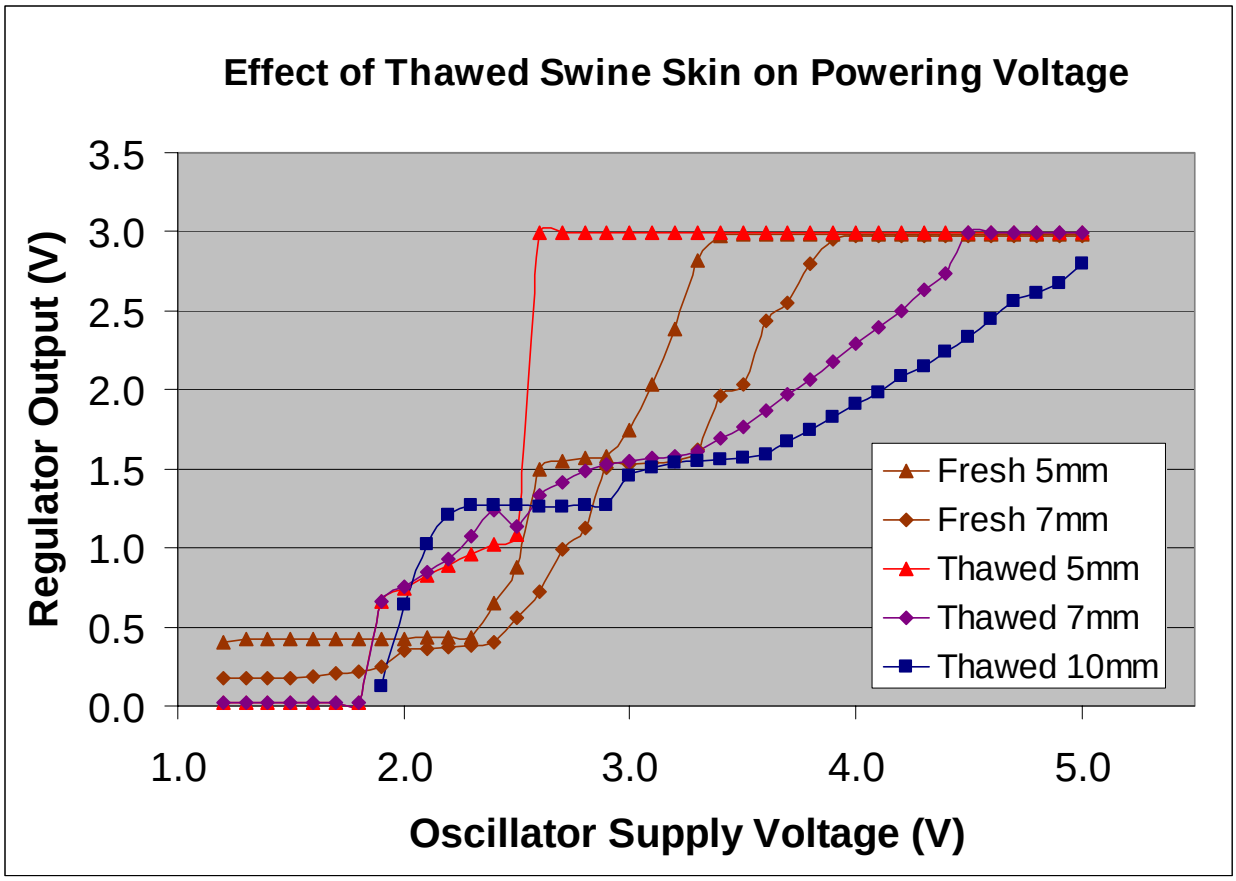

Figure 28: Plot of maximum regulator output voltage vs. oscillator voltage using thawed swine skin.

5.3 CADAVER SCALP TESTING RESULTS

The plot of regulator output voltage against oscillator supply voltage through the cadaver scalp is shown in Figure 29. Also shown on the graph are the results of the same test performed through air for comparison purposes.

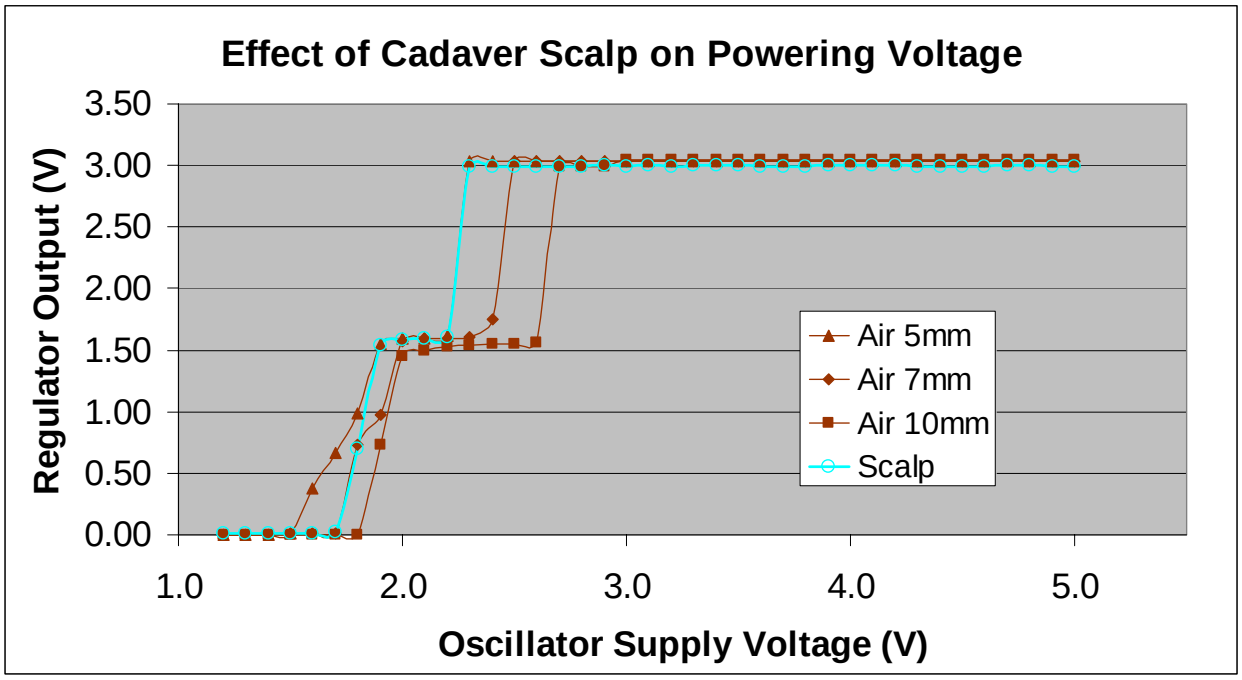

Figure 29: Plot of maximum regulator output voltage vs. oscillator voltage using cadaver scalp.

Figure 30 presents the results of the transmitter coil distance test.

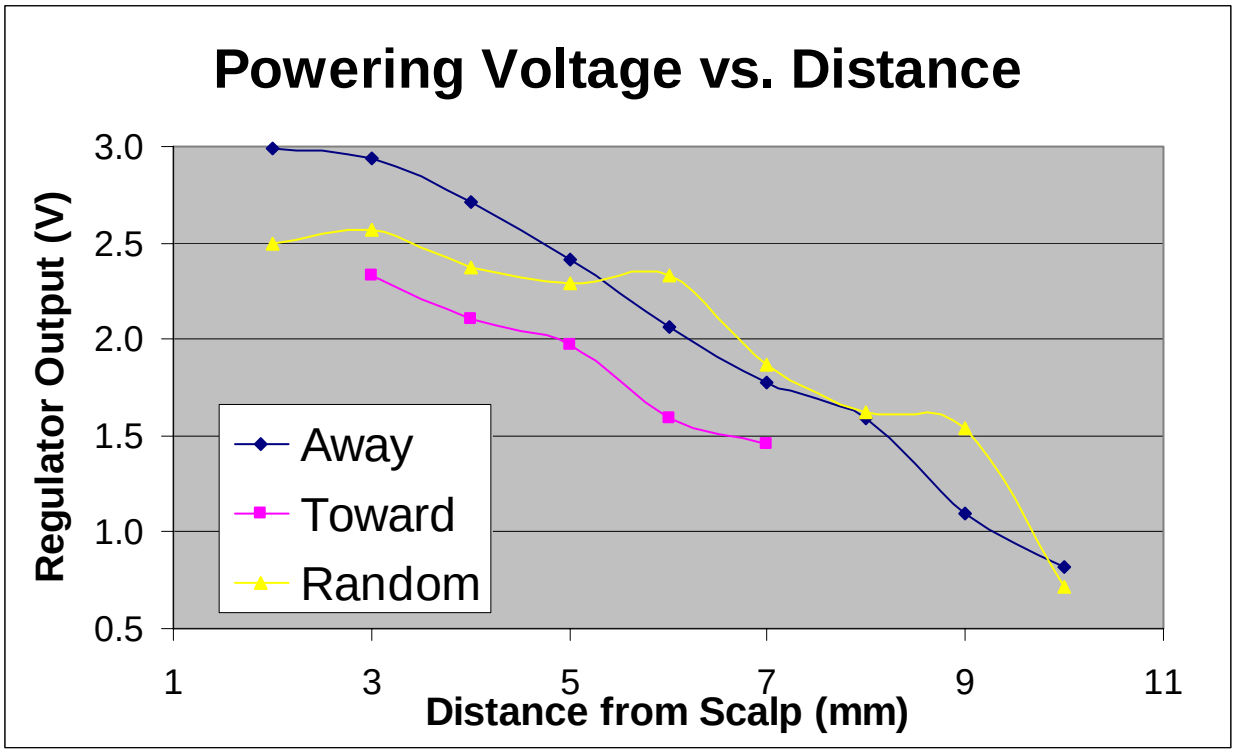

Figure 30: Plot of regulator output voltage vs. distance between transmitting coils and scalp.

6.0 DISCUSSION OF RESULTS

This chapter contains the analysis of the testing results presented in Chapter 5.0.

6.1 TESTING THROUGH AIR

6.1.1 Powering and Programming

As can be seen in Figure 24, the voltage regulator driving the control circuitry can easily provide the 3 volts necessary with a transmitting coil oscillator voltage less than 3 volts, even at a distance of 10 millimeters. The powering of the oscillator with 4.5 volts, well above the drop-off range, can easily be accomplished with three standard AAA batteries. For the two shorter distances, the energy transfer is fairly efficient, as the 3 volts necessary to drive the control circuitry can be attained with only 2.5 volts on the external coil. The intermediate plateau seen on all three curves, almost halfway between 0 volts and the maximum voltage, is common in all similar tests of the device. This is most likely due to the geometry of the coils on the PCB. As the near-field gets weaker with diminishing oscillator supply voltage, its field constricts, excluding the outermost receiving coils from the equipotential field lines first. This accounts for the sharp drop in voltage. Because the four innermost receiving coils are still mostly within the field, a steady voltage is maintained, the plateau on the graph. Further constriction of the field with decreasing oscillator supply voltage cuts out the rest of the receiving coils, hence the final drop decreasing towards 0 volts.

6.1.2 Powering Mechanism

This test was performed to resolve any question about the exact mechanism of the power transfer. Some doubt may be expressed as to the inductive coupling of the actual coils, with other possible power source candidates being the attached measurement wires or even a hidden battery. However, modifying only the coil, i.e. eliminating it as a possible source, removes the regulator output voltage seen otherwise. Hence, the coil around the control circuitry PCB can be considered to be the actual receiver of the near-field energy transmission.

6.2 TESTING THROUGH SWINE SKIN

The swine skin experiments serve as a rough indicator or analog of the device performance through actual human skin. Figure 27 shows a shift of the voltage curves to the right from those from testing through air. This implies that the transmitted signal must be stronger for the secondary coil to receive the same amount of energy. This is not surprising, given that the intervening skin is expected to attenuate the signal. However, even 4 volts is a high enough oscillator supply voltage to produce the required 3 volts for the control circuitry, so a simple scheme of using three AAA batteries is still completely viable.

However, Figure 28 showing the graphed results from the thawed skin is not as promising. This experiment also more closely resembles that of the cadaver scalp, being that the skin has been frozen and thawed. The 5-mm thick skin shows surprisingly good results after being thawed, better than those of the fresh skin. This is most likely due to a decrease in the

amount of moisture in the skin. Some attenuation still exists, but a mere 2.5-volt supply on the oscillator is enough to drive the control circuitry. Testing with the 7- and 10-mm pieces of skin, however, produces not only a shift to the right, but also a deformation of the curve. The only difference between these pieces of skin and the 5-mm piece, besides thickness, is the presence of a subcutaneous layer of fat, which had coagulated through the freezing and thawing process. If the 5-mm piece of skin, with an absence of any fat, is an indicator that the skin itself attenuates less after freezing and thawing, then the fat cells attached to the 7- and 10-mm pieces must attenuate more after the same process. This explains the relatively large shift of the curves for the thicker pieces of skin. One can speculate that the deformation of the curve is caused by a deformation of the inductive coupling field, which may be caused by the more pronounced difference in attenuation factors between the fat cells and surrounding tissue and air. Despite the relatively poor performance of the 7- and 10-mm pieces of skin, for which a 4.5-volt oscillator supply is almost enough, four AAA batteries, supplying 6 volts, can be expected to be sufficient to power the device while remaining small and easily replaceable.

6.3 TESTING THROUGH CADAVER SCALP

The cadaver scalp experiment clearly proves the viability of the remotely powered implant. Despite the skin being dead, it is the closest model to a live human scalp out of all the tests performed. Figure 29 shows that the energy transfer through the scalp is almost equivalent to that of energy transfer through 5 millimeters of air, as if the scalp were not even present. Some speculation may exist as to whether the movement of the ionic fluids in living tissue would attenuate the signal more. Given the relatively low frequency typically used in these experiments, approximately 14 MHz, any attenuation due to fluid movement can be expected to

be negligible. Because an oscillator supply voltage of 2.5 volts is enough to provide the internal circuitry with its required power, the small and simple three AAA battery setup previously mentioned will supply plenty of power for the device.

The second cadaver scalp experiment results detailed in Figure 30 may be misleading upon first inspection. This test was done in a rapid manner, disallowing the relatively slow charging and discharging voltage multiplier to keep up with the varying distance. Note that the distance measured is the separation between the transmitting coil and the scalp. Assuming the scalp to be a minimum of 5 millimeters thick and accounting for the roughly 3 millimeters of electric sealant on the implant, the actual distance between coils is 8 millimeters longer than that on the graph. Additionally, the oscillator frequency was not varied at any distance step in order to produce maximum output voltage. As the transmitting coil was pulled away from the scalp, the input voltage to the regulator (output voltage of the charge pump) dropped slowly, creating the smooth curve which is slightly higher than the static output voltage at each distance. For similar reasons, the curve created upon decreasing the distance is lower than that of a supposed static output voltage curve, because the charge pump does not have enough time to charge fully. The third plot, created by taking measurements at random distances in sequence, is more sporadic than the other two, as would be expected. For example, placing the coil directly from a 5-mm separation to a 9-mm separation would result in a higher voltage output at 9 mm than if the separation had been increased slowly. This is because the charge pump has not discharged fully from its state at 5 mm. Explanations aside, this particular experiment stresses the need for a slight improvement in the energy transfer scheme to allow for adjustments of the powering coil position over the scalp in the final prototype.

7.0 DEMONSTRATION OF PROTOTYPE IN A MODEL OF ACTUAL USAGE

Proof of concept, though bolstered by experimental data, would not be complete without a means of implementation. Parkinson's disease is not only a physical affliction; it is also a social disease. The main problem with current implants is the subcutaneous wiring and large battery pack. However, they still remain inconspicuous under the skin. The device detailed in this research requires an external power source on top of the scalp in addition to the implant under the scalp, begging the question, "How is the device implemented in a socially acceptable manner?"

In answer to such a question, a model head has been fitted with a DBS prototype, scalp covering and powering hat to demonstrate an aesthetically pleasing implementation of the entire device. The head is a simple Styrofoam head model on top of which the circuitry is embedded. Wires for measuring the pulse outputs and control circuitry supply voltage run down through the head and out the back of the neck. A custom-designed ABS Plastic scalp model fits on top of the head to cover the implant. The hat is a basic driver's hat with the transmitting coil and three AAA batteries. The model is fully functional according to the specifications in Table 1. Figure 31 shows how the model fits together and how it looks when assembled.

Figure 31: Prototype implementation model showing (a) components and (b) fully assembled.

8.0 CONCLUSIONS

A simplified deep brain stimulation device has been developed and tested. The device is remotely powered via inductive coupling, consuming just over 10 joules per day. The implantable circuitry fits on a 1.2-in. square PCB with a maximum thickness of ¼ in. Experiments through air, porcine skin and a cadaver scalp have proven the effectiveness of the powering and programming schemes. Additionally, the power transmitting coil can be driven via a small, cheap and easily replaceable external battery pack. A model has been made to demonstrate a feasible realization of the entire device which is both functional and aesthetically pleasing.

9.0 FUTURE WORK

The project completed to this point forms a foundation for further development of the remotely powered implant. Having proven the ability to power and program such a small device, the remaining work consists of optimizing its components, both minimizing power consumption and maximizing energy transfer, implementing more stimulation profile flexibility, and creating an implantable substrate to house the circuitry.

Looking at the energy usage calculations from Section 3.1.3, one can see the bulk of the power is dissipated in the microcontroller and most especially the voltage regulator. With advancing technology, the voltage regulator is replaceable with newer devices requiring about one tenth of the power, which could cut overall energy usage drastically. The microcontroller is likely replaceable with newer, lower power devices, perhaps from a different manufacturer.

In the context of powering the device, many changes can be made to improve performance. The transmitting and receiving coils used in the current prototype are in no way optimized. As described in Section 3.2, the coil layout used is simply the best of four tested configurations. Research into optimization of the coil design to minimize losses could greatly improve performance. Optimization of the charge pump as well has the potential to reduce losses further. Eventually, energy harvesting technology will be integrated into the device, allowing storage of energy over periods of time when the device is not in use. This as well could help provide a more efficient use of transmitted power.

Before the device can possibly be used to administer DBS treatment, its pulsing parameter flexibility must be increased. This flexibility is necessary both before and after the

brain probe is implanted. Different people respond slightly differently to the treatment, so the pulsing parameters for any one person are customized for best results. After implantation, pulsing is often modified to compensate for biological adjustments to the treatment. Additionally, the device could ultimately be used to administer DBS for afflictions besides the targeted Parkinson's disease. Extended flexibility can come from code modifications adding more frequency and duration settings, as well as the implementation of a digital-analog converter to control pulsing amplitude. A DAC will allow for a significantly greater number of amplitude settings than the presently used static voltage divider scheme. Along with adding more variability, a method for storing the pulsing parameters while the device is not powered needs to be developed. The current prototype loses all programmed information upon losing power, which is certainly a possible situation with regular usage.

The flexible substrate to house the circuitry for actual implantation is currently being researched by a startup company in Pittsburgh. This substrate must be thin, flexible, biocompatible, and electrically neutral.

As with any large project, the doors for future research are wide open, presenting much opportunity and future promise.

APPENDIX A

CONTROL CIRCUITRY MICROCONTROLLER CODE

```
// Steven A. Hackworth, Parkinson's (Brain Cap) Project
// Last Updated: March 28, 2005

// Code for microcontroller in the implant, including control
// and receiving programming instructions
#include <16F87.h>
// #fuses set in Configure -> Configuration Bits... menu from MPLab
#use delay(clock=125000)
#use fast_io(A)
#use fast_io(B)

void SetDefaults(int & pulse, int & amp, int & dur, int & freq);
void GetParameters(int & pulse, int & amp, int & dur, int & freq);
void SetProbeValue(int value);
void SetAmplitudeValue(int & amp, int value);
void SetDurationValue(int & dur, int value);
void SetFrequencyValue(int & freq, int value);
void SetPulsingState(int & pulse, int value);

void main()
{
      int pulse, amp, dur, freq;
      // pulse: 0 = pulsing off, 1 = pulsing on
      // amp: 0 - 128 tells which output pin B0 - B7 (and hence which voltage
divider)
      //   to pulse, allowing for scaling of output voltage in eight steps
      // dur: 0, 1, 2 = 120, 180, 60 us pulse widths
      // freq: 0 - 1 = lowest - highest frequency

//// register values:
//    WDTCON = 0x5
//    OSCCON = 0xF
//    STATUS = 0x3
//  OPTION = 0x1

      // select bank 1 for OSCCON register (set bit 5 of the STATUS reg)
      // internal oscillator set to 125 kHz from default of 32 kHz (set bit 4
of OSCCON reg)
      // clear PS<0> and PS<2> of the OPTION reg for 1:4 prescaler
      // select bank 2 for WDTCON register
      // clear WDTPS2 bit in the WDTCON register
```

```
      //   on power-up, the register defaults to ---01000, making the WDT
prescaler 1:512
      //   clearing the 1 makes the prescaler 1:32, giving the WDT a period
of 1 ms
      #asm
            BSF 0x3,0x5
//          BSF 0xF,0x4  // comment out this line to leave INTRC at 32 kHz so
the 8 MHz osc won't turn on
            BCF 0x1,0x0
            BCF 0x1,0x2
            BCF 0x3,0x5
            BSF 0x3,0x6

            BCF 0x5,0x3
            BCF 0x3,0x6
      #endasm

      set_tris_a(0x60);  // PIN_A5, PIN_A6 are inputs, rest are outputs
      set_tris_b(0x00);  // all B pins are outputs

      output_high(PIN_A4);  // reset the RF receiver chip
      delay_cycles(2);
      output_low(PIN_A4);


      output_b(0);

      SetDefaults(pulse, amp, dur, freq);

      while(TRUE)
      {
            if(!input(PIN_A5))  // programming signal present (data from
ATA5283 low)
                  GetParameters(pulse, amp, dur, freq);  // get and set
parameters

            if(pulse == 1)  // pulse if it's supposed to pulse
            {
                  if(dur == 1)  // 180 us pulse duration
                  {
                        if(freq == 1)  // higher frequency
                        {
                              delay_cycles(2);
                              output_b(amp);
                              delay_cycles(5);
                              output_b(0);
                        }
                        else           // lower frequency
                        {
                              delay_cycles(5);
                              output_b(amp);
                              delay_cycles(5);
                              output_b(0);
                        }
                  }
                  else
                  {
```

```
                        if(dur == 0)  // 120 us pulse duration
                        {
                              if(freq == 1)  // higher frequency
                              {
                                    output_b(amp);
                                    delay_cycles(3);
                                    output_b(0);
                              }
                              else           // lower frequency
                              {
                                    delay_cycles(3);
                                    output_b(amp);
                                    delay_cycles(3);
                                    output_b(0);
                              }
                        }
                        else        // 60 us pulse duration
                        {
                              if(freq == 1)  // higher frequency
                              {
                                    delay_cycles(3);
                                    output_b(amp);
                                    delay_cycles(1);
                                    output_b(0);
                              }
                              else           // lower frequency
                              {
                                    delay_cycles(6);
                                    output_b(amp);
                                    delay_cycles(1);
                                    output_b(0);
                              }
                        }
                  }

/* this is code for static 185 Hz timing with 4 duration settings
                  if(dur >= 2)
                  {
                        if(dur == 3)
                        {
                              output_b(amp);
                              delay_cycles(7);
                              output_b(0);
                              delay_cycles(2);  // for 185 Hz timing
                        }
                        else
                        {
                              output_b(amp);
                              delay_cycles(5);
                              output_b(0);
                              delay_cycles(4);  // for 185 Hz timing
                        }
                  }
                  else
                  {
                        if(dur == 1)
                        {
```

```
                              output_b(amp);
                              delay_cycles(3);
                              output_b(0);
                              delay_cycles(6);  // for 185 Hz timing
                        }
                        else
                        {
                              output_b(amp);
                              delay_cycles(1);
                              output_b(0);
                              delay_cycles(8);  // for 185 Hz timing
                        }
                  } */
            }


            // select bank 2 for the WDTCON register
            // enable the WDT (set SWDTEN)
            #asm
                  BSF 0x3,0x6
                  BSF 0x5,0x0
                  BCF 0x3,0x6
            #endasm

            sleep();  // to wake up after WDT timeout

            // select bank 2
            // disable the WDT (clear SWDTEN)
            #asm
                  BSF 0x3,0x6
                  BCF 0x5,0x0
                  BCF 0x3,0x6
            #endasm
      }
}

void SetDefaults(int & pulse, int & amp, int & dur, int & freq)
// Initializes the device to pulse at a frequency of ~185 Hz
// Pulses are ~120 us and almost Vdd to probes 1 and 2
{
      SetProbeValue(12);  // probes 1 and 2 turned on

      SetAmplitudeValue(amp, 3);  // output highest voltage step

      SetDurationValue(dur, 0);  // pulse width of ~120 us

      SetFrequencyValue(freq, 0);  // lower frequency

      SetPulsingState(pulse, 1);  // pulsing on
}

void GetParameters(int & pulse, int & amp, int & dur, int & freq)
// Checks for a programming signal.  If present, it sets the desired
parameters
//   to the desired values
// The programming signal pre-header is long enough that this microcontroller
//   will see it before the official header starts
```

```
// Currently, only one parameter can be changed at a time.
{
      int type, value;

      while(!input(PIN_A5))  // wait for end of pre-header
      {
            delay_cycles(1);
      }

      // wait 64 us
      delay_cycles(2);

      /* check header */

      if(input(PIN_A5))  // check for 1
      {
            delay_ms(2);
      }
      else
      {
            delay_ms(30);
            output_high(PIN_A4);  // Reset the receiver chip
            delay_cycles(2);
            output_low(PIN_A4);
            goto end;
      }
      if(!input(PIN_A5))  // check for 0
      {
            delay_ms(2);
      }
      else
      {
            delay_ms(30);
            output_high(PIN_A4);  // Reset the receiver chip
            delay_cycles(2);
            output_low(PIN_A4);
            goto end;
      }
      if(input(PIN_A5))  // check for 1
      {
            delay_ms(2);
      }
      else
      {
            delay_ms(30);
            output_high(PIN_A4);  // Reset the receiver chip
            delay_cycles(2);
            output_low(PIN_A4);
            goto end;
      }
      if(!input(PIN_A5))  // check for 0
      {
            delay_ms(2);
      }
      else
      {
            delay_ms(30);
```

```
      output_high(PIN_A4);  // Reset the receiver chip
      delay_cycles(2);
      output_low(PIN_A4);
      goto end;
}


/* header okay, now get parameter type */

if(input(PIN_A5))  // MSB
      type = 4;
else
      type = 0;

delay_ms(2);

if(input(PIN_A5))
      type += 2;

delay_ms(2);

if(input(PIN_A5))  // LSB
      type += 1;

delay_ms(2);


/* type received, now get parameter value */

if(input(PIN_A5))  // MSB
      value = 8;
else
      value = 0;

delay_ms(2);

if(input(PIN_A5))
      value += 4;

delay_ms(2);

if(input(PIN_A5))
      value += 2;

delay_ms(2);

if(input(PIN_A5))  // LSB
      value += 1;


delay_ms(8);
output_high(PIN_A4);  // Reset the receiver chip
delay_cycles(2);
output_low(PIN_A4);

/* change the appropriate parameter */
```

```
	switch(type)
	{
		case 0: SetProbeValue(value);  // 000 sets which probes
			break;

		case 1: SetAmplitudeValue(amp, value);  // 001 sets amplitude
			break;

		case 2: SetDurationValue(dur, value);  // 010 sets duration
			break;

		case 3: SetFrequencyValue(freq, value);  // 011 sets frequency
			break;

		case 4: SetPulsingState(pulse, value);  // 100 sets pulsing
on/off
			break;

		default:
			break;
	}

	end: return;
}

void SetProbeValue(int value)
{
	if(value >= 8)  // MSB corresponds to probe 1
	{
		output_high(PIN_A0);
		value -= 8;
	}
	else
	{
		output_low(PIN_A0);
	}

	if(value >= 4)  // probe 2
	{
		output_high(PIN_A1);
		value -= 4;
	}
	else
	{
		output_low(PIN_A1);
	}

	if(value >= 2)  // probe 3
	{
		output_high(PIN_A2);
		value -= 2;
	}
	else
	{
		output_low(PIN_A2);
	}
```

```
	if(value >= 1)  // LSB corresponds to probe 4
	{
		output_high(PIN_A3);
		value -= 1;
	}
	else
	{
		output_low(PIN_A3);
	}
}

void SetAmplitudeValue(int & amp, int value)
{
	switch(value)
	{
		case 0: amp = 0x01;
			break;

		case 1: amp = 0x02;
			break;

		case 2: amp = 0x04;
			break;

		case 3: amp = 0x08;
			break;

		case 4: amp = 0x10;
			break;

		case 5: amp = 0x20;
			break;

		case 6: amp = 0x40;
			break;

		case 7: amp = 0x80;
			break;

		default: amp = 0x00;
			break;
	}
}

void SetDurationValue(int & dur, int value)
{
	dur = value;
}

void SetFrequencyValue(int & freq, int value)
{
	freq = value;
}


void SetPulsingState(int & pulse, int value)
```

```
// sets pulsing state on if value is 1, off otherwise
{
	if(value == 1)
		pulse = 1;
	else
		pulse = 0;
}
```

APPENDIX B

PROGRAMMING CIRCUITRY MICROCONTROLLER CODE

```
// Steven A. Hackworth, Parkinson's (Brain Cap) Project
// Last Updated: January 30, 2005

// Code for controlling transmission of 125 kHz signal
// for programming the control circuit

#include <16F87.h>
#fuses // all taken care of in the Configure -> Configuration Bits... menu
#use delay(clock=8000000)
#use FAST_IO(A)
#use FAST_IO(B)

int getType();
void SendHeader();
void SendType(int type);
void SendValue(int value);
void Pulse2ms();

void main()
{
      int type,value;

      // select bank 1 for OSCCON register (set bit 5 of the STATUS reg)
      // internal oscillator set to 8 MHz from default of 32 kHz (set bits 4-
6 of OSCCON reg)
      #asm
            BSF 0x3,0x5
            BSF 0xF,0x4
            BSF 0xF,0x5
            BSF 0xF,0x6
            BCF 0x3,0x5
      #endasm

      set_tris_a(0xFF);
            // port A is all inputs
      set_tris_b(0xEF);
            // B0-B3,B5-B7 = pins 6-9,11-13 are inputs
            // B4 = pin 10 is an output

      while(TRUE) // always running
      {
```

```
            if(input(PIN_B3)) // high input on pin 9
            {
                  type = getType();
                  value = input_a();
                  SendHeader();
                  SendType(type);
                  SendValue(value);
                  delay_ms(500);
            }
      }
}

int getType()
// only one of pins 6-8,11-12 should be high at this stage AND
// one of pins 6-8,11-12 must be high at this stage
{
      if(input(PIN_B0))  // pin 6 = which probes
      {
            return 0;
      }
      else
      {
            if(input(PIN_B1))  // pin 7 = amplitude
            {
                  return 1;
            }
            else
            {
                  if(input(PIN_B2))  // pin 8 = duration
                  {
                        return 2;
                  }
                  else
                  {
                        if(input(PIN_B5))  // pin 11 = frequency
                        {
                              return 3;
                        }
                        else
                        {
                              if(input(PIN_B6))  // pin 12 = pulse on/off
                              {
                                    return 4;
                              }
                        }
                  }
            }
      }

      return 5;
}

void SendHeader()
{
      int i;

      for(i=1;i<=4;i++)  // receiver chip wakeup >5.6 ms
```

```
            Pulse2ms();

      delay_ms(8);  // make sure PIC sees the signal >5.4 ms

      Pulse2ms();     // 1
      delay_ms(2);    // 0
      Pulse2ms();     // 1
      delay_ms(2);    // 0
}

void SendType(int type)
// sends coded signal for which parameter will be programmed
{
      switch(type)
      {
            case 0: delay_ms(2);  // which probes = 000
                        delay_ms(2);
                        delay_ms(2);
                  break;

            case 1: delay_ms(2);  // amplitude = 001
                        delay_ms(2);
                        Pulse2ms();
                  break;

            case 2: delay_ms(2);  // duration = 010
                        Pulse2ms();
                        delay_ms(2);
                  break;

            case 3: delay_ms(2);  // frequency = 011
                        Pulse2ms();
                        Pulse2ms();
                  break;

            case 4: Pulse2ms();  // pulse on/off = 100
                        delay_ms(2);
                        delay_ms(2);
            default:
                  break;
      }
}

void SendValue(int value)
// sends coded signal for value of parameter needing to be changed
{
      if(value >= 8)    // MSB, 1st 2 ms
      {
            Pulse2ms();
            value -= 8;
      }
      else
      {
            delay_ms(2);
      }

      if(value >= 4)    // 2nd 2 ms
```

```
	{

		Pulse2ms();
		value -= 4;
	}
	else
	{
		delay_ms(2);
	}

	if(value >= 2)    // 3rd 2 ms
	{
		Pulse2ms();
		value -= 2;
	}
	else
	{
		delay_ms(2);
	}

	if(value == 1)    // LSB, 4th 2 ms
	{
		Pulse2ms();
	}
	else
	{
		delay_ms(2);
	}
}

void Pulse2ms()
// creates 125 kHz square wave for 2 milliseconds
{
	int i;

	for(i=1;i<=250;i++)
	{
		output_high(PIN_B4);  // pin 10 goes high for 4 microseconds...
		delay_cycles(7);
		output_low(PIN_B4);  // then pin 10 goes low for 4 microseconds
//		delay_cycles(1);  // this NOP combined with the loop control
makes 4 us
	}
}
```

APPENDIX C

VOLTAGE MULTIPLIER CIRCUIT OPERATION

This appendix contains an explanation of the underlying mechanism in a voltage multiplier. A voltage multiplier takes an AC voltage as input then multiplies and rectifies it into a higher DC voltage. A voltage multiplier can have one or multiple stages, each one acting as a basic voltage doubler. Figure 32 shows the basic voltage doubler stage, composed of two capacitors and two diodes.

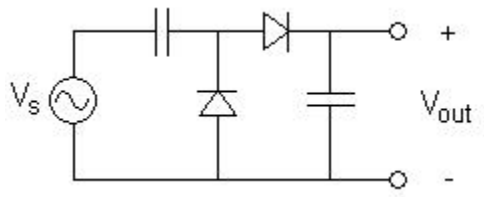

Figure 32: The basic voltage doubler stage.

The voltage doubler must be analyzed in two stages, one for each phase of the AC input. Figure 33 shows the circuit during the first phase of the input. The vertical diode in Figure 32 acts as a short circuit, while the horizontal diode acts as an open circuit. This puts the first capacitor, or "flying" capacitor, in parallel with the input. Its voltage is thus equal to the input voltage V in the polarity indicated.

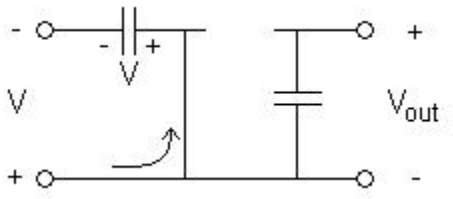

Figure 33: First phase of the voltage doubler cycle.

When the input switches polarities the model circuit changes slightly. The two diodes switch roles, the vertical one acting as an open circuit and the other acting as a short circuit. See Figure 34. Because the voltage across the flying capacitor can't change instantaneously, it holds its original voltage V. This voltage is in series with that of the input, thus creating 2V across the output capacitor, doubling the voltage.

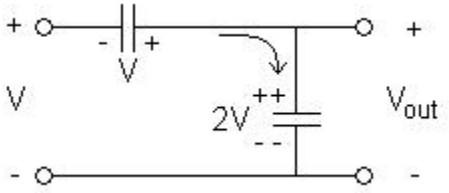

Figure 34: Second phase of the voltage doubler cycle.

As stated earlier, multiple stages can be connected in series, each one essentially doubling the output voltage of the stage before. However, a practical limit exists due to losses in the components and conservation of power. The higher voltages at later stages can drive less of a load due to a reduction in the current, thus attaching a load usually drops the actual voltage output.

The input to a voltage multiplier can have an effect on its efficiency. Square waves produce better results than other waveforms due to their almost instantaneous phase transitions.

These allow less time for the capacitors to leak charge. A higher frequency works better for the same reasons, though only up to a certain point. The capacitors need enough time for a net gain in voltage from charging each phase. Due to charging time, the output voltage sometimes rises (or drops) very slowly after application of the input voltage. This phenomenon is seen during the distance tests performed with the cadaver scalp in Section 5.3.

APPENDIX D

FINDING L AND C RESONANT VALUES FOR PROGRAMMING TRANSMITTER

The governing equation for calculating inductor and capacitor values in a resonant circuit is:

$$\omega_o = 2\pi \cdot f_o = \frac{1}{\sqrt{LC}}$$

Equation 2: Formula relating resonant frequency to L and C values.

Using Equation 2, a frequency of 125 KHz corresponds to an LC product of 1.62×10^{-12}. Choosing a capacitor value of 1 μF necessitates the use of a 1.62-μH inductor. Given standard component values and tolerances, the decision was made to use a 1.6-μH inductor with a 1-μF capacitor for the programmer's resonant circuit.

BIBLIOGRAPHY

[1] About Parkinson Disease:
http://www.parkinson.org.

[2] Gálvez-Jiménez, Néstor, Ed. *"Scientific Basis for the Treatment of Parkinson's Disease Second Edition"* Taylor & Francis, Boca Raton, 2005.

[3] Pahwa, Rajesh, et al, Ed. *"Handbook of Parkinson's Disease Third Edition"* Marcel Dekker, Inc., New York, 2003.

[4] O Lüders, Hans, Ed. *"Deep Brain Stimulation and Epilepsy"* Taylor & Francis, Independence, 2004.

[5] Correspondence with Douglas Kondziolka, MD, MS, FRCS (C), Professor of Neurological Surgery and Radiation Oncology, UPMC.

[6] Microchip. "PIC16F87/88 Data Sheet," 2003.

[7] Atmel. "Interface IC for 125 kHz Wake-up Function: ATA5283 Preliminary," 2004.

[8] Maxim. "Low-Cost, Low-Voltage, Quad, SPST, CMOS Analog Switches: MAX4066/MAX4066A," 1996.

[9] Correspondence with Varghese John, E-SOC, Inc.

[10] Linear Technology. "300mA Low Dropout Regulators with Micropower Quiescent Current and Shutdown: LT1521/LT1521-3/LT1521-3.3/LT1521-5," 1995.